UNIVERSITY OF OKLAHOMA

GRADUATE COLLEGE

THE ENIGMATIC QUATERNARY SHELL BED DEPOSITS OF LAKE TANGANYIKA, TANZANIA: LINKING ANTHROPOGENIC LAND-USE WITH NEARSHORE SEDIMENTATION

A THESIS

SUBMITTED TO THE GRADUATE FACULTY

in partial fulfillment of the requirements for the

Degree of

MASTER OF SCIENCE

By

JAMES FRANCIS BUSCH
Norman, Oklahoma
2017

THE ENIGMATIC QUATERNARY SHELL BED DEPOSITS OF LAKE TANGANYIKA, TANZANIA: LINKING ANTHROPOGENIC LAND-USE WITH NEARSHORE SEDIMENTATION

A THESIS APPROVED FOR THE
CONOCOPHILLIPS SCHOOL OF GEOLOGY AND GEOPHYSICS

BY

_____
Dr. Michael Soreghan, Chair

_____
Dr. Gerilyn Soreghan

_____
Dr. Kirsten de Beurs

Acknowledgements

This work was funded by the National Science Foundation (grant EAR- 1424907). We also thank the DigitalGlobe Foundation for providing proprietary satellite imagery data for the study; Colin Apse and Dan Kelly (The Nature Conservancy) for their support in sharing GIS data and providing consultation; the Tanzania Fisheries Research Institute (TAFIRI) for their support and collaboration; Mupape Mukuli, Patrick Ryan, Joseph Lucas, and Anna Gravina for their assistance and collaboration in the field.

Table of Contents

List of Tables

List of Figures

Abstract

Extensive deposits of carbonate shell-rich sediments in the nearshore environment (< 30 m water depth) of Lake Tanganyika, Africa, form a unique and important habitat for a diversity of endemic crabs, fish, sponges, and bryozoa. Anthropogenically-induced alteration of the hinterland from deforestation, burning of land, and agricultural activities threaten this crucial habitat through sediment pollution of the littoral environment. In the Mahale Mountains region (Tanzania), we examined the sedimentology of the shell-beds to test whether their heterogeneity is related to onshore disturbances within three moderately-sized watersheds (> 100 km^2). Here, we suggest that observed onshore watershed disturbances result in sediments that are muddier with a higher percentage of clay in the area offshore of the Lagosa and Rukoma river watersheds compared to the area offshore of the largely unaltered Katumbi river watershed. Widespread burning of land, agricultural land-use, and the torrential rains of the wet season are causal factors that result in significant increases in fine-grained clastic sedimentation, increased fluvio-deltaic sediment plume size, and increased delta shoreline progradation. In areas most affected by sedimentation, littoral sponges are largely absent, and we speculate that other important benthic organisms that inhabit the shell beds are also negatively impacted by the influx of fine-grained clastic sediment. The discovery of a small population of *Neothauma tanganyicense* offshore of the relatively unaltered Katumbi river watershed suggests that the shell beds' heterogeneity could be related to anthropogenic land-use and its effect on the occurrence of shell-bed forming gastropods.

Introduction

Lake Tanganyika, located within the East African Rift, (*Figure 1*) is the world's largest tropical rift lake, and the second largest lake in the world by volume (McGlue et al. 2010). Lake Tanganyika is bordered by Burundi, the Democratic Republic of the Congo, Tanzania, and Zambia and serves as an important natural resource for all four countries. In addition to containing over 1500 species of plants and animals, many of which are endemic, Lake Tanganyika is the only modern tropical lacustrine depositional system to have a diversity of carbonate facies similar to lacustrine carbonates observed in the geological record (Coulter 1991; Cohen and Thouin 1987). Of the many carbonate facies observed in Lake Tanganyika, arguably one of the most important for hosting the diverse and numerous lake taxa are the shell beds.

The shell beds of Lake Tanganyika are death assemblages that blanket the shallow, nearshore environment and are composed of whole shells, shell fragments of varying size, and clastic sediment (*Figure 2*) (Soreghan and Cohen 1996; McGlue et al. 2010; Soreghan 2016). Important to note is that extensive modern shell beds are absent from all other East African lakes, and living specimens of the gastropod species which compose the shell beds are absent from the modern shell beds of Lake Tanganyika (McGlue et al. 2010). Significant spatial variability in the shell beds' sedimentologic characteristics have been documented by previous studies noting substantial differences in shell composition and sediment texture with changes in both depth and geographic location in the littoral environment (Soreghan and Cohen 1996; McGlue et al. 2010; Soreghan 2016). Results from these studies have established a connection between physical processes in the littoral environment and sedimentological attributes of the

shell beds, where lateral differences in shell-bed composition might reflect interaction with fluvio-deltaic sedimentation and past lake-level changes.

Furthermore, other internationally funded organizations concerned about the health and conservation of the lake's fisheries completed studies in the 1990's (e.g. Lake Tanganyika Biodiversity Project- LTBP) identified deforestation and soil erosion as one of the major threats to the lake's ecosystem (Cohen et al. 1996; Patterson, 2000). However, most studies examining the effects of anthropogenic sedimentation on the nearshore environments of Lake Tanganyika have focused primarily on rocky habitats, rather than the wide, shallow littoral platforms where shell beds occur (Cohen et al. 1993b; Alin et al. 1999; Donohue and Irvine 2004; McIntyre et al. 2005; Cohen et al. 2005). Therefore, our study focuses on how coupled deforestation and soil erosion affect the littoral shell-bed environment on the shallow, hinged platforms, as they likely differ from rocky environments in aquatic species composition, lake floor gradients, and possibly adjacent land-cover types.

In order to better determine the impacts of recent anthropogenically-induced sedimentation and its potential impact on the shell-bed ecosystem, it is critical to document spatial differences in sediment patterns across an area exhibiting varying intensity of human alteration. Specifically, the goal of this study is to compare watersheds of varying anthropogenic alteration and quantitatively tie observations made onshore to sediment composition offshore in the Mahale Mountains region of Lake Tanganyika, Tanzania. We aim to test the hypothesis that there is a correlation among the amount of onshore disturbance in a watershed, the sediment texture offshore of the

watershed, the progradation rate of the watershed's shoreline, and the abundance and health of benthic aquatic fauna in the nearshore environment.

This study integrates remote sensing analysis, observational and sedimentologic data, and multivariate statistical techniques to assess possible connections between anthropogenic alteration of watersheds adjacent to Lake Tanganyika and the composition of shell beds in the littoral environment. The shell beds cover hundreds of square kilometers of the shallow littoral environment of Lake Tanganyika and serve as the key habitat for many of the endemic fish, crab, sponge, and mollusk species which inhabit the lake (Cohen and Thouin 1987; Cohen 1989a; Soreghan and Cohen 1996; McGlue et al. 2010; Soreghan 2016). Therefore, a better understanding of how watershed disturbances have impacted shell-bed composition and benthic communities in recent time is important to guide conservation policies designed to protect nearshore environments from future degradation. Furthermore, the study has implications for biologists interested in how the rate and magnitude of different types of environmental change affect community structure and range shifts of aquatic organisms tied to the shell-bed substrate.

Background

Geological History and Limnology of Lake Tanganyika

The formation of the East African Rift System and its numerous lacustrine basins began in the Miocene, when extensional deformation created a network of elongate-shaped rift basins (Rosendahl et al. 1986; Cohen et al. 1993a). Lake Tanganyika formed between 9-12 Ma (Cohen et al. 1993a) and is divided into two main basins (north and south), separated by the Kalemie-Mahali bathymetric shoal (Rosendahl et al. 1986; Lezzar et al. 1996). High angle, basin bounding faults border the lake, which comprises several opposite polarity half grabens (*Figure 1*) (Rosendahl et al. 1986; Cohen et al. 1993a; Lezzar et al. 1996; McGlue et al. 2008). Lake Tanganyika is 650 km long with an average width of 50 km, and is approximately 1470 m deep in the southern basin and averages 570 m depth (O'Reilly et al. 2003).

The water of Lake Tanganyika is relatively fresh and less alkaline in comparison to most other East African lakes, but importantly has high Mg and Ca concentrations as well as a high Mg/Ca ratio (Cohen 1989b; Casanova and Hillaire-Marcel 1992) resulting in a water chemistry particularly conducive to the precipitation of calcium carbonate. The overwhelming majority of the lake's water volume is anoxic; the average depth of the oxycline is roughly 150 m (Hecky and Degens 1973; Coulter and Spiegel 1991), but is subject to fluctuation during the dry season when differential cooling of the lake and stronger winds promote upwelling of nutrient-rich anoxic waters into the epilimnion (Verburg et al. 2011). However, Lake Tanganyika is classified as a meromictic, oligotrophic lake that is permanently stratified (Coulter 1991; Plisnier et al. 1999).

Lake Tanganyika is hydrologically open, with minimal water loss through the westward draining Lukuga River (*Figure 1*). Most water loss from the lake occurs through evaporation due to a relatively warm (20-24 ºC mean annual temperature) and monsoonal climate (Hecky and Degens 1973; Coulter and Spiegel 1991). The wet season (~October-April) is generally warmer, less windy, and accounts for almost all of the annual precipitation received by the region (~1000 mm mean annual precipitation) (O'Reilly et al. 2003). The dry season (~May-September), by comparison, is cool with persistent southeasterly winds, and receives almost no precipitation (Verburg et al. 1997; O'Reilly et al. 2003; Verburg et al. 2011).

Sedimentological Characteristics of the Shell Beds of Lake Tanganyika

The dominant shell types that compose the shell beds are *Neothauma tanganyicense*, a viviparid gastropod, and *Coelatura sp*., a unionoid clam. Several of the endemic cichlid fish species actively modify the shell beds to build nests or use the shells themselves to hide and brood young, and diverse sponge morphs use the shells as a substrate with which to anchor themselves (Coulter 1991). Previous researchers have noted that the shell beds of Lake Tanganyika show significant variability in shell taphonomy, constituent mollusk species, and clastic sediment fraction with changes in water depth and geographic location (Cohen and Thouin 1987; Cohen 1989a; Soreghan and Cohen 1996; McGlue et al. 2010; Soreghan 2016).

Most researches have noted that the shell beds are confined to the littoral to sub-littoral zone of Lake Tanganyika on the shallow platform margins (Cohen and Thouin 1987; Cohen 1989a; Soreghan and Cohen 1996; McGlue et al. 2010). McGlue et al. (2010) identified three dominant shell-bed facies found in the littoral zone of Lake

Tanganyika: (1) gravel-rich mollusk hash, (2) sandy and silty mollusk hash, and (3) pure mollusk hash. The occurrence of each of the three facies correlates with lake-floor gradient and water depth, suggesting that reworking of shells by wave energy, fluctuations of lake level, and incorporation of fluvio-deltaic sediments are the primary mechanisms that produce the different facies (McGlue et al., 2010). Radiocarbon dating of surface shells in the same study indicate that at least some shells have persisted over the last 1000+ years, supporting the notion that shell beds have formed a significant component of the lake's substrate through recent time.

Spatially, the shell beds occur as laterally continuous bands concentrated mostly between 12 and 30 m water depth. The shell beds are discontinuous where fluvio-deltaic sediments have been deposited proximal to the river mouth, blanketing the shells with primarily mud. The shell beds' occurrence in laterally continuous, thin bands overlying clastic sediment is interpreted as resulting from either (1) winnowing and reworking of shell beds during moderate lake-level lowstands, or (2) reworking of shells by a change in wave base during transgression (Cohen 1989a; McGlue et al. 2010).

The life histories of the shell-bed gastropods in Lake Tanganyika, primarily *N. tanganyicense* and *Coelatura sp.,* are poorly understood, largely because live specimens are extremely rare (Soreghan and Cohen 1996; McGlue et al. 2010; Soreghan 2016). Coulter (1991) concluded that *Coelatura sp.* are shallow, infaunal, filter feeders that inhabit mixed substrates. Previous observations documented that *N. tanganyicense* generally inhabit clear, shallow waters with sandy and silty substrates (Moore 1903; Leloup 1953; McGlue et al. 2010). West et al. (1991) observed that juvenile snails bury themselves 3-10 cm deep in soft substrate to avoid predators. Van Damme and Pickford

(1999) suggested that adult African viviparids do not burrow like the juveniles, but rather use a probiscus to feed on endobenthic organisms while living on the surface of the sediment.

Recent molecular phylogenetic studies concluded that *N. tanganyicense* snails existed in Africa since the early to middle Miocene (5-15 Ma), coincident with significant extension and subsidence in the Tanganyika Basin (Sengupta et al. 2009). Thus, their persistence in Lake Tanganyika is thought to be long lived and an important component of the littoral ecosystem and its biodiversity. However, their absence as live organisms in the modern environment has led researchers to investigate whether it could reflect either ***1)*** recent and rapid human-induced changes to the littoral ecosystem, or perhaps ***2)*** natural basin-wide environmental change triggering widespread mortality of *N. tanganyicense*.

Land-Use Change, Sedimentation, and Aquatic Fauna in Lake Tanganyika

The deleterious effects of sediment pollution on aquatic ecosystems have been documented in many watersheds around the globe (e.g. Donohue and Molinos 2009), and previous studies of Lake Tanganyika have demonstrated that anthropogenic-induced sedimentation is responsible for decreased diversity of fishes, ostracods, and mollusks (Cohen et al. 1993b; Alin et al. 1999; Alin et al. 2002; Donohue et al. 2003; Donohue and Irvine 2004; McIntyre et al. 2005). Donohue and Irvine (2004) subjected live gastropods to varying levels of sedimentation in both laboratory aquariums and in Lake Tanganyika, and measured their response in body weight and survivorship. The results indicated that, for the larger gastropods, mortality increased when subjected to increased sedimentation. However, McIntyre et al. (2005) found that when evaluating

assemblage-level metrics of gastropods at locations of varying anthropogenic perturbation in Lake Tanganyika, there was little evidence of changes in species richness, evenness, or snail abundance at the levels of sedimentation recorded in the study. At the individual level, however, snails at impacted sites ingested large amounts of inorganic sediments and were associated with a decreased size distribution, suggesting gastropods have a more complex response to increased sedimentation than previously thought.

Paired historical records and sediment cores collected from Lake Tanganyika suggest that as early as the late-18th to early-19th centuries widespread deforestation, colonization, and agricultural operations were affecting watersheds in the hinterland (Alin et al. 2002; Cohen et al. 2005). In the Mahale Mountains region, significant increases in sediment accumulation rates did not occur until the mid-20th century, suggesting that widespread watershed disturbance in rural, more remote areas, lagged the urban localities further north and are a more recent phenomenon (Cohen et al., 2005). However, for more recent time not necessarily recorded in sediment cores and historical records, it is desirable to accurately quantify the amount and type of onshore disturbance that has occurred within a watershed in order to determine the degree to which onshore activities have affected the littoral ecosystem in both the modern and historical context. One effective method of doing this is through multispectral satellite imagery analysis, and although previous studies have attempted to correlate land-use change with increased sediment load and sediment yield in watersheds of varying alteration (Donohue et al. 2003), to date, no studies have attempted to draw correlations between anthropogenically-induced alteration to watersheds identified in satellite

imagery, changes in sedimentation offshore, and the shell-bed ecosystem of Lake Tanganyika.

Methods

The field work for this study was carried out at Lake Tanganyika in July-August of 2015 and 2016 and was conducted from the Tuungane field station near Buhingu, Tanzania. Field and laboratory data collection methods are outlined below, followed by GIS and remote sensing and statistical methodology.

Field Methods

Sampling Transects

Within the Mahale Mountains study area, sampling transects were established at varying proximity to the major river deltas and towns and oriented perpendicular to the shoreline (*Figure 3*).

Shell Sample Collection

Bulk shell samples were collected by navigating a boat to the sampling transects using a Lowrance HDS-5 sonar unit to locations at 20, 15, 12, and 9 m water depth. A GPS point was recorded using the sonar unit once the anchor had been dropped and the boat had stopped drifting. At each depth sampling location, two researchers used SCUBA to randomly place a 50 cm x 50 cm quadrant on the lake bottom. If shells were present within the quadrant, all shells were collected and placed in a mesh sampling bag. If shells were not present at the surface, but shells were felt underneath a thin sediment blanket, the shells were excavated by hand and collected but noted as sub-surface samples. If no shells were felt within the top 2-3 cm of the sediment surface, the sample was marked as lacking shells. Once back at the field station, the shells were dried and placed in labeled plastic bags.

Sediment Sample Collection

Along each transect, sediment samples were also collected at depths of 20, 15, 12, 9, 6, and 3 m. GPS points were collected in the same manner described above for each sample location, and two researchers descended to the lake floor using SCUBA. A plastic sampling jar was pressed into the lake floor sediment and the lid was slid under the jar to fully capture the sediment volume. At the surface, the sediment (and any water) from the containers was transferred into plastic sampling bags. Once back at the field station, the bags were opened to allow excess water to evaporate.

For water depths exceeding reach using SCUBA, a PONAR sampler was deployed from the boat to collect sediment samples. PONAR sampling was done along each transect at 30 and 40 m depths. If shells were caught in the PONAR jaws during retrieval, the sample was recollected to ensure an unbiased sample.

Photographic Underwater Surveys

At each location, where sediment and shell samples were collected, photographs of the substrate were taken using a GOPRO camera. At 15, 12, 9, and 6 m water depth, photographic surveys of the lake floor were also taken to characterize the benthic organisms and substrate. The surveys were completed by placing the 50 cm x 50 cm quadrant on the lake floor, taking a picture from directly above the quadrant, and then flipping the quadrant forward to repeat the process. This was done such that the photographic transect was 10 m long (20 photographs).

Sidescan Sonar Collection

Sidescan sonar was collected using the Lowrance HDS-5 sonar unit with a StructureScan attachment. The settings used for the data collection were as follows: 200

khz frequency channel, a range of 55 m, scrolling speed of 1/2x, low noise rejection, and low surface clarity settings. Lines were collected along the sampling transects, as well as parallel to shore at constant depths of 6, 9, 12, 15, and 20 m such that the sidescan lines intersected the sample locations for each transect.

Bathymetry Data Acquisition

Bathymetry data were collected for a region encompassing the Mahale Mountains study area by Dr. Michael McGlue (University of Kentucky) during the 2015 field season.

Sponge Abundance Calculation

Sponge abundance was determined by using the ten best consecutive images for each photographic transect and counting all the sponges visually distinguishable within each quadrant for a given image. The number of sponge occurrences was then recorded.

Shell Bed Percent Cover Calculations

Shell bed percent cover was computed using Adobe Illustrator by first creating an artboard with equal dimensions to the quadrant (50 cm x 50 cm). Then, each image was resized such that the quadrant lined up exactly with the artboard. Afterwards, the areas in the image where shells were present (whole shells or obvious shell fragments) were outlined using the pen tool. After all the areas containing shells were outlined, a script was used to compute the total area in the image containing shell material. This area was then divided by the total area of the quadrant to compute the percent of the total area considered as shell-bed substrate. The method was repeated for the ten best consecutive images for each photographic transect.

Laboratory Methods

Weight % Grain Size

Sediment samples were analyzed for weight percent of gravel, sand, and mud by wet sieving the bulk sediment sample through #14 (1410 μm) and #230 (63 μm) sieves. Prior to the sieving, samples were split in half: one half was archived in a sample bag and the other was placed in a beaker with deionized (DI) water. Samples in the beaker were then placed on a hot plate at 65º C and 10 mL of 30% H_2O_2 was added to each beaker. After 24 hours, an additional 10 mL of H_2O_2 was added to each beaker. Following another 24-hour period, the sample was rinsed in DI water and sieved. The gravel (material caught on the #14 sieve) and sand (material caught on the #230 sieve) fractions were dried and weighed. For the mud fraction, the mud and water that passed through the sieves were retained in a bucket and transferred into a 1000 mL beaker. The beaker was then filled to the 800 mL mark using DI water, stirred very rapidly, and a 10 mL vial was used to extract a small sample for additional grain size analysis. Afterwards, the mud beaker was allowed to settle for 24 hours, excess water was pipetted out of the beaker, and the sample was dried and weighed. A data table summarizing the results is included in Appendix E.

Loss On Ignition (LOI) Estimation of Organic Matter

From the archived bulk sample, a 2-4 g sub-sample was extracted and placed in a small beaker. The sample was then dried and transferred to a pre-weighed crucible. After each sample was transferred to the crucible, the samples were placed in a furnace at 550º C for 4 hours. After the 550-degree burn, the crucibles were weighed and then placed back in the furnace at 900º C for an additional 4 hours. Following the 900-degree

burn, the crucibles were weighed again and the sample was discarded. A data table summarizing the results is included in Appendix F.

Laser Particle Grain Size Analysis

The 10 mL vials containing the sub-sampled mud fraction for each sample were analyzed for grain size with a Malvern Mastersizer 3000 laser diffraction particle grain size analyzer (LPSA). The specific methods used for operating the LPSA are included in Appendix A, and a data table summarizing the results is included in Appendix G.

GIS and Remote Sensing Methods

Landsat Images

Landsat images of the Mahale Mountains study area were downloaded from the USGS Earth Explorer data acquisition platform. All images were preprocessed by the USGS to their Level-1 (L1T) product level and are described at length in the Landsat 8 Data Users Handbook (2016, and references therein). The USGS surface reflectance data products were not used in this study because of major processing artifacts in our study area resulting from inaccuracies with their method when large bodies of water are present in image scenes. At least two images for the dry season (~June-September) and two images for the wet season (~October-May) were downloaded for each year of the entire Landsat archive, if there were enough images of acceptable quality during each season of the year. Images were considered to be of acceptable quality if clouds did not obscure the major river deltas and watersheds in the study area. Scene ID's, acquisition dates, sensor information, and path/rows of each image acquired are included in Appendix D.

DigitalGlobe Images

As a part of the DigitalGlobe Foundation's imagery grant program, 10 high-resolution images collected by DigitalGlobe's proprietary satellite constellation were acquired. All images were delivered as Standard 2A Imagery products, which were radiometrically corrected, sensor corrected, and projected to a plane using a UTM map projection and WGS-84 datum. Standard imagery also has a coarse Digital Elevation Model (DEM) applied to it, which is used to normalize for topographic relief with respect to the reference ellipsoid. All standard imagery products have uniform ground sample distance (GSD) throughout the entire product.

Image Processing

For the purpose of calculating the Normalized Difference Vegetation Index (NDVI) and the Normalized Burn Ratio (NBR), an atmospheric correction was performed on the Landsat images using Exelis ENVI software. The atmospheric correction was performed on each raw Landsat image using ENVI's Quick Atmospheric Correction (QUAC) tool with the predefined settings specific to Landsat imagery.

Climate Data Acquisition

Rainfall data were acquired from NOAA's Climate Prediction Center International Desk Data Archive. The Africa RFE 2.0 (rainfall estimate) Daily Total was chosen as the most appropriate product and was downloaded in raster format for 2001 (oldest data available) until 2016. The spatial resolution of RFE 2.0 data is 0.1º (12.8 km).

Land Cover, Watershed, and Elevation Data Acquisition

Land cover data (2001-2014), watershed boundaries and rivers, and a digital elevation model (DEM) for the study area were supplied by The Nature Conservancy (TNC). The three largest watersheds in our study area (Katumbi, Lagosa, and Rukoma) were selected for comparison, although, it should be noted several smaller watersheds are situated between them in the study area (*Figure 3*). For each of the three largest watersheds in the study area, the slope was computed from the DEM and the areas for each of the land cover types were calculated. Elevation data were compiled from NASA's SRTM mission, and the methods used by Daniel Kelly (TNC) for classifying land cover type are included in Appendix B.

Rainfall Statistics for the Mahale Mountains Region

The daily rainfall estimations from the RFE 2.0 product were summed for every day of each month within the Mahale Mountains region using the Cell Statistics Tool in ArcMap. The Mahale Mountains region was traced into a shapefile using a municipal boundary that extends north to Kigoma, Tanzania using ArcMap's basemap, which displays the borders and municipalities of Tanzania. The summed rainfall raster was then projected into the UTM 35 S coordinate system, and the Extract by Mask tool was used to isolate the rainfall data only within the Mahale Mountains region. Finally, the average was taken of each monthly rainfall summary and recorded in a table.

Sediment Plume Area Calculations

Raw L1T Landsat images, rather than the atmospherically corrected images, were used for the analysis because of known limitations of the QUAC atmospheric correction tool for imagery scenes over open water. The principal components were

computed for each image using Arcmap's Principal Component tool (the number of principal components is equal to the number of spectral bands for each image) in order to spectrally distinguish areas of turbid water associated with the sediment plumes from non-turbid water. Then, an Iso-Cluster Unsupervised Classification was performed on each principal component image using the following parameters: 50 classes, minimum class size of 20 for Digital Globe images and 4 for Landsat images. The classified principal component images were then visually compared to the plume visible in the multispectral images, and the classes that best delineated the sediment plumes were isolated. Using the Raster Calculator tool, a Boolean statement was then written that selected only the pixels within the sediment plume if they were correctly classified in all of the principal component images. The Tabulate Area tool was then used to compute the total area of each sediment plume, and the values were recorded in a table along with observations about the visual characteristics of each plume.

Normalized Burn Ratio Calculations

The atmospherically corrected Landsat images were used as the input into the Normalized Burn Ratio (NBR) equations in accordance with the accepted methodology outlined by the Fire Effects Monitoring and Inventory Protocol (FIREMON 2004): $NBR = \frac{SWIR2-NIR}{SWIR2+NIR}$; $\Delta NBR = NBR_{prefire} - NBR_{postfire}$ where SWIR is the second short wave infrared band and NIR is the near infrared band. The ΔNBR images were then classified into seven classes, where the class with the highest values represents the high-severity burn land cover (FIREMON 2004). The cutoff values for the high-severity burn classification were determined by examining actively burning land present in the imagery, so that the most recently burned land could be used as a ground-truth location

to visually assess the accuracy for the high-severity burn class and the cutoff values could be modified as needed. The high-severity burn class was then used to calculate the total area of land burned within each of three major watersheds in the study area.

NDVI Calculations

The atmospherically corrected Landsat images were used as inputs into the equation for the Normalized Difference Vegetation Index (NDVI): $NDVI = \frac{NIR-Red}{NIR+Red}$ where NIR is the near-infrared band and Red is the red band for each Landsat image. After the NDVI was computed, the values were extracted for each of the three watersheds in the study area, and the average NDVI value for each of the watersheds was recorded in a table.

Shoreline Mapping and Progradation Calculations

Using Landsat images, the near-infrared band was used as an input into Arcmap's Slope tool (percent rise) to map the maximum rate of change for the pixel values at the water-land interface. The slope image was then classified into 25 classes using the Jenks Natural Breaks method. Afterwards, the classified slope image was reclassified such that the class values would be reversed (largest values reassigned to be the smallest values). The reclassified slope image was then used as an input into the Cost Distance tool, and the cost distance and backlink rasters were used with the Cost Path tool (best single method) to compute the "least cost path" across the image, which is equivalent to the shoreline. Each computed "least cost path" was then converted from a raster to a polyline feature using the Raster to Polyline Feature tool. Accuracy of the shorelines was visually assessed, and when there were minor errors in the shoreline

mapping, the polyline was manually edited to accurately represent the shoreline location.

In order to compute the distance that each shoreline had prograded from the oldest mapped shoreline (1984), the Euclidean Distance tool was used to create a distance raster from the 1984 shoreline location, which was mapped using the least cost path method described above. The Zonal Statistics tool was then used to calculate the mean distance that each shoreline had moved from the 1984 shoreline location. The amount of error for the shoreline distance calculation was determined by summing the pixel size and geometric error, which are both included in each image's metadata.

Statistical Methods

Hypothesis Testing

For the summary statistics of the sediment plume area, NDVI, NBR, and LPSA results, a two-tailed t-test ($\alpha = 0.05$) was used to determine if statistically significant differences existed between two populations of samples. Pairwise comparisons consisted of the Katumbi and Lagosa, the Katumbi and Rukoma. and the Rukoma and Lagosa watersheds. Prior to the t-test, an F-test was completed to determine if the two variables for each t-test did in fact have equal variances, and depending on the results, a two-tailed t-test assuming either equal or unequal variances was used.

Principal Component Analysis (PCA)

Principal component analysis (PCA) was performed on the data collected for all samples including the following variables: depth, mud weight %, grain-size mode of the mud fraction, and distance to adjacent delta. The data were normalized using a Z-score normalization with the standard deviation (Abdi and Williams 2010), and imported as a

matrix of values into Matlab. In Matlab, pairwise correlation was checked between the variables to ensure that they were correlated above an acceptable threshold (~0.30), and the principal components were computed using the PCA function. The coefficients of the principal components were then transformed to be orthonormal and used to compute the component scores. Biplots were then created for PC1 and PC2, and PC2 and PC3 to visualize relationships between each variable's loading values and their correlation with the principal components.

Results

The results section is structured such that the data from the suite of analyses performed on the sediment samples is presented first, followed by the underwater photographic surveys. Then, the results of the GIS analyses are discussed, and lastly the principal component analysis results are presented.

Grain Size Data

Sediment samples collected across the study area vary with respect to the mud (< 63 μm) and gravel (< 1410 μm) fractions at 3, 6, 9, 12, 15, and 20 m water depths (*Figure 6*). Generally, transects adjacent to the deltas exhibit the highest percentages of mud. At 3 m, the samples are uniformly sandy, but there is significant mud (ranging 6 to 51%) nearest the Lagosa and Rukoma deltas (TLA, T15, T2, T5). At 6-12 m water depths, similar trends occur, wherein transects nearest the deltas have higher proportions of mud (up to 75%), and the more distal transects contain more gravel (up to 90%). At 15 and 20 m water depth, samples are muddier at the Katumbi and Lagosa deltas (23-76%), but not the Rukoma delta (5-7%). Samples from 30 and 40 m water depth are generally less muddy across all transects (ranging 0 to 46%), with the northern transects (north of T7) proximal to the Lagosa and Rukoma deltas composed of less than 13% mud.

LOI based Organic Carbon and Inorganic Carbon Data

The 550º C loss on ignition (LOI) values estimate the amount of organic carbon contained in a sediment sample. In samples measured from 15, 20, and 30 m water depth (*Figure 7*), the values range from 0.9 to 8.2% and generally increase across the study area from south (~2%) to north (~3.5%) for all depths; however, no apparent

relationship occurs between LOI values and water depth. At 15 m water depth, LOI is more variable, with significant increases at the Katumbi (T10) and Lagosa (T2) river mouths, but not the Rukoma River mouth (T5). At 20 m water depth, there are similar increases in LOI at the Katumbi (T11) and Lagosa (T15) deltas, but of a lesser magnitude. For 30 m water depth, there is less variability and no significant spikes in LOI, but rather a more gradual increase in values from south (2.2%) to north (3.0%).

The 900º C LOI values estimate the amount of inorganic carbon contained in a sediment sample, and are more variable among water depths (ranging 0.7 to 40%) (*Figure 8*). At 15 m, the carbonate-based LOI is generally low across the study area, with higher values occurring between T7 and T1 (ranging 17-26%). At 20 and 30 m water depths, carbonate-based LOI is high south of the Katumbi river mouth at T13 (17-18%), very high between the Katumbi river mouth and the Lagosa river mouth (26-38%), and high adjacent to the Rukoma river mouth (11-40%).

Laser Particle Grain Size Analysis

The mud fractions of the bulk sediment samples (< 63 μm) were analyzed for their size distribution using LPSA. The mode of the size distribution was chosen to best represent the grain size of the mud fraction, because in some instances non-normal distributions skewed the mean grain size. The mode of the mud fraction (*Figure 9*) displays some variability at 15, 20, and 30 m water depth (ranging from 6 to 54 μm), but generally fines from south to north for all water depths. At 15 m, the mud is coarser south of the Katumbi river mouth (50-52 μm), fines to less than 15 μm at T1, becomes coarser at T14 (51 μm), and is very fine north of T2 (14 μm). For 20 m water depth, the trend is very similar, with coarser mud occurring adjacent to the Katumbi river mouth

(53-55 μm), but fining north to <15 μm at T6; the mud coarsens again to 43 μm at T14 and again fines north of T2 to < 12 μm. The mode of the mud fraction at 30 m is also coarser adjacent to the Katumbi river mouth (43-50 μm) but fines to 6 μm at T14; it also coarsens north at transect TLA (33 μm) and then fines again toward T4 (10 μm).

Percent clay (material < 3.9 μm) was computed from the LPSA data for all samples at 15, 20, and 30 m water depths, and shows a general increase in values from SW to NE among all depths (ranging 2 to 22%) (*Figure 17*). At 15 m, the % clay increases irregularly from a minimum of 2% near the Katumbi river (T12) to a maximum of 12 % at the Lagosa river mouth (T15) and remains higher at the Rukoma river mouth (T5, 8%). The samples from 20 m display a similar trend, with minimum % clay at T12 (2%), maximum values at the Lagosa river mouth (T15, 13%), and higher values at the Rukoma river mouth (T5, 10%). At 30 m, the clay % shows the greatest range in values, with a minimum clay content of 3% near the Katumbi river at T11, maximum values of 22% at the Lagosa river mouth (T14), and modest clay near the Rukoma river at T5 (5%).

For onshore samples collected from the river channels and from overbank environments, results from a t-test indicate that those near the Katumbi river delta have a statistically significant higher average modal grain size (M = 33.7, SD = 13.1) than those near the Lagosa river delta (M = 20.4, SD = 14.3) ($t(27) = -2.42$, $p = 0.02$). However, results from a t-test examining the % clay in the onshore samples found no statistically significant difference between those adjacent to the Katumbi river delta (M = 2.94, SD = 1.86) and the Lagosa river delta (M = 6.87, SD = 11.10) ($t(9) = 1.06$, $p = 0.32$).

Sponge Abundance Data

Sponge occurrences range from 0 to 155 in the water depths where we had complete photographic coverage across the transects (12 and 15 m) (*Figure 4*). Both water depths display similar trends, with coincident decreases occurring adjacent to the Katumbi, Lagosa, and Rukoma river deltas. Abundances at the sampled transects nearest the three river mouths ranged from 0 to 2 (# per transect) for both depths, whereas transects to the north of Katumbi river and to the south of Lagosa river show higher abundances (ranging from 3 to 155).

Shell Bed % Cover Data

Average shell-bed cover for 12 and 15 m water depth ranged from 0 to 100% (avg % area per transect) (*Figure 5*). Both water depths display very similar changes in values moving from south to north. At 12 m water depth, the substrate consists almost exclusively of shells, except where proximal to the river mouths at T9, T2, and T5. The substrate at 15 m water depth displays a nearly identical trend as that exhibited at 12 m, where the substrate consists almost entirely of shell material, with the exception of T5 (23%).

Land Cover Summary (2001-2014) and Watershed Characteristics

The Katumbi watershed is the smallest of the three watersheds (drainage basin of 112 km^2), but has the highest elevation in the study area (avg elevation 2501 m) and thus a steeper topographic gradient (average slope of 19º) (*Table 1*). The most extensive land cover type in the watershed is evergreen forest, which covers nearly half of the watershed (48 km^2), and includes forests that occur at higher elevations in more humid conditions (*Table 2*). Miombo, a low elevation sub-humid forest, and herbaceous land

cover compose most of the other half of the watershed area, with a minor portion of mixed agriculture (primarily cassava and maize). The Lagosa and Rukoma watersheds are more similarly sized, significantly larger (242 and 314 km^2), occur at lower elevations (average elevations of 1878 and 1905 m), and have more gentle slopes (average slopes of 8 and 10º) than the Katumbi watershed. They also contain similar land cover types, with miombo forest making up nearly half of both watersheds. The second most important land cover type in the watersheds is bamboo, followed by mixed agriculture.

Rainfall Data

The average monthly rainfall from 2001-2015 in the Kigoma region (*Table 3*) displays a characteristically dry season from May to September, when almost no rainfall occurs, and then a wet season from October-April, when almost all rainfall for the year occurs. In 2003 and 2005, there was significantly less rainfall than the mean annual rainfall (MAR), and in 2004. 2006, 2009, and 2011, there was significantly more rainfall than the MAR.

Sediment Plume Area Calculations

Sediment plumes were classified and the areas for each computed for all imagery available for the wet season. A full summary of the calculations and plume descriptions are included in Appendix C. Image dates ranged from 1991 to 2016, and there was no observable trend in the plume size through time. A t-test of the average size of the sediment plumes in images acquired during the wet season (n = 13) shows a statistically significant difference between those that occurred at the Katumbi river delta (M = 0.08 km^2, SD = 0.18) and those observed at the Lagosa (M = 1.92 km^2, SD = 0.69)

(t(14) = 8.92, p = 3.78E-07) and Rukoma (M = 2.58 km^2, SD = 0.97) (t(12) = 8.39, p = 2.3E-06) river deltas. Even during the peak of the wet season, in most cases there was either little to no observable sediment plume emanating from the Katumbi river delta, or the plume was not large or dense enough to be detected in the imagery. In contrast, the plumes identified from the Lagosa and Rukoma river deltas are on average quite large, with no statistically significant difference between them (t(23) = 1.90, p = 0.07). Generally, the Lagosa river plume is partially deflected to the northeast, where it hugs the shoreline, and partially deflected into a small embayment to the southwest, where it is broadly dispersed (*Figure 10*). The Rukoma river plume displays more variable directionality, but was often deflected to both the east and to the west depositing sediment over a broader area.

NDVI and NBR Calculations

The vegetation density and health was examined by computing the normalized difference vegetation index (NDVI) for the study area in both the wet and dry seasons (higher NDVI values = more dense and/or healthier vegetation). In the wet season, t-test results indicate that there is not a statistically significant difference between the NDVI of the three watersheds. However, in the dry season the Katumbi watershed (M = 0.71, SD = 0.09) maintains higher mean NDVI values that are statistically significant than either the Rukoma (M = 0.57, SD = 0.13) (t(32) = -3.43, p = 0.002) or the Lagosa (M = 0.55, SD = 0.13) (t(32) = -3.86, p = 0.001) watersheds.

The total area of land burned in the study area watersheds was estimated using the normalized burn ratio (NBR). For the years during which the NBR was calculated (*Table 4*), a t-test demonstrated that there is a statistically significant difference in the

total area of land (km^2) burned in the Katumbi (M = 4.4, SD = 2.3), Lagosa (M = 54.4, SD = 33.4) (t(7) = 3.95, p = 0.006), and Rukoma (M = 37.7, SD = 14.9) (t(7) = 5.83, p = 0.001) watersheds. In the Katumbi watershed, minimal burning occurred between 1995 and 2016; however, large areas in the Rukoma and Lagosa watersheds were burned regularly (*Table 4*) during the same period with no statistically significant different between the Rukoma and Lagosa watersheds (t(10) = 1.21, p = 0.25).

Shoreline Progradation Calculations

Using the oldest (1984) satellite images, the mean distance of shoreline progradation was calculated for every year that imagery could be acquired until 2016. All river shorelines prograded significant distances between 1984 and 2016, but the progradation rate was non-linear (*Figure 11*). By 2016, the Rukoma and Lagosa rivers prograded higher mean distances (96 ± 23 m and 82 ± 23 m, respectively) than the Katumbi river (37 ± 23 m). The Rukoma and Lagosa rivers experience an increase in the progradation rate between 2004 and 2007; however, the Katumbi river does not experience the same increase in progradation rate over the same time period.

PCA Results

Principal component analysis was performed on four variables for each sediment sample: water depth, distance from adjacent delta mouth, mode of mud grain size fraction, and mud weight % of bulk sample. The results of the PCA indicate principal components 1-3 account for most of the variance (89.5%) in the data (*Table 5*). PC1 accounts for the majority of the variance in the data (45%), while PC2 (22.9%) and PC3 (21.6%) account for nearly equal amounts of the remaining variance. For the PC1 vs. PC2 biplot (*Figure 12*), the depth and distance to adjacent delta variables load

positively on PC1, while the mode of mud and mud % negatively loaded on the PC1 axis (*Table 6*). The distance to adjacent delta variable accounts for most of the variance in PC1. The mode of mud, depth, and distance to adjacent delta are positively loaded on PC2, whereas the mud % is negatively loaded on PC2. The mode of mud variable accounts for most of the variance in PC2. The Katumbi samples tend to cluster on the positive side of PC2, suggesting a correlation with the grain-size mode of the mud fraction of the bulk sediment samples, while the Rukoma and Lagosa samples cluster on the negative side of PC2, resulting in a correlation with the mud weight % of the bulk sediment sample.

The PC2 vs. PC3 biplot (*Figure 13*) shows nearly identical results and clustering of samples as the PC1 vs. PC2 biplot, but the contribution of each variable to the principal components is slightly different. The mud % and depth load positively on PC3, whereas distances to adjacent delta and mud size modes exhibit little correlation with PC3. The water depth variable accounts for most of the variance observed in PC3, but does not differentiate between sample location with respect to the three deltas.

Discussion

Our study's approach makes use of both remotely sensed data to characterize onshore land disturbances and sedimentologic data collected from the offshore shell-bed environment of Lake Tanganyika north of the Mahale Mountains to constrain how sedimentation processes and identified disturbances within the study area's watersheds impact the littoral shell-bed habitat. Our survey suggests that documented spatial differences in the texture and composition of clastic sediment as well as the density and nature of the shells themselves correlate to differences in anthropogenically-induced alteration within three watersheds. The data from our study shows that for watersheds more intensively affected by recent burning and have more agricultural land-use, the sediments offshore of the watersheds are muddier and finer-grained, the occurrence of sponges is lower or nonexistent, the shell-bed substrate is absent (likely covered by the fluvio-deltaic muds), and the sediment plumes emanating from the deltas of affected watersheds are significantly larger than the unaffected watershed. Our study also implemented multivariate statistics in order to determine if samples offshore of the unaffected and affected watersheds could be distinguished from one another using sedimentologic and physical parameters. PCA successfully discriminated samples offshore of the impacted watersheds from those adjacent to the unaffected Katumbi watershed, suggesting that intra-watershed processes onshore are responsible for the observed differences offshore.

Variation in Sedimentologic Data

The weight-percent grain size data, grain-size mode of the mud fraction, and % clay of the samples indicate that offshore sediments derived from the Lagosa and

Rukoma rivers have a higher percentage of mud, and the mud fraction is finer-grained compared to those adjacent to and at the mouth of the Katumbi river (*Figure 14*). The Katumbi river sediments are characterized by a more significant gravel and coarse sand component with less clay (composed of clasts/grains of metamorphic basement rock, pers. obs., 2015), as well as significant terrestrial organic matter in the form of plant leaves, sticks, and even full-sized tree trunks (pers. obs., 2015) (*Figures 6, 7, and 17*). By contrast, the Lagosa and Rukoma samples are characterized by finer-grained sediments with a higher percentage of clay, and are largely devoid of the larger-sized terrestrial plant detritus, but contain a more significant amount of fine-grained particulate organic matter (pers. obs., 2015) (*Figures 6, 7, and 17*). Descriptions of the gravel fraction of the samples reveals that the Katumbi river not only has a more significant amount of clastic gravel (rather than shell material), but also much more large, terrestrial organic matter. Although the LOI organic carbon results suggest that the Lagosa river delta has more organic matter contained in the sediments, the data could reflect methodological bias since many pieces of terrestrial plant detritus characteristic of Katumbi river sediments are too large to fit in the crucible used for the LOI testing. Thus, the LOI data from the Katumbi river samples might underestimate the organic matter content.

The PCA of the offshore sediments adjacent to the river deltas successfully discriminated samples offshore of altered watersheds from those located near the unaltered Katumbi watershed, and shows that the grain-size mode of the mud fraction exhibits the highest loading value among the four principal components (*Figures 12 and 13, Table 6*).

Onshore Disturbance and Potential Impacts on Offshore Sedimentation

Onshore disturbance was characterized using satellite imagery analysis in order to interpret vegetation abundance and health (NDVI) and patterns of large-scale burning of vegetation (NBR). These metrics were then linked with offshore sedimentation through the identification and areal computation of fluvio-deltaic sediment plumes, which should relate directly to suspension deposition and the consequent mud content of the offshore surface sediments.

The sediment plumes imaged at the Lagosa and Rukoma rivers are on average 1.8 km^2 and 2.5 km^2 larger, respectively, than the plumes imaged at the Katumbi river (*Figure 10*). The primary controls on the existence of a sediment plume are the relative density differences of the river and lake water, and the effective grain size of the suspended sediment, which dictates sediment settling velocities (Geyer and Kineke 2004). Consequently, in this case, when there is no appreciable difference in the wave/wind conditions or in the temperature or density of the lake waters across the study site, the size of a sediment plume emanating from the three rivers can be loosely correlated with the suspended sediment load entering the lake. Averages of plume size computations over a long time period (1991-2016) should then provide an excellent proxy for the differences in sediment load grain size between the three rivers in our study area. Thus, the larger sediment plumes associated with the Rukoma and Lagosa rivers are interpreted to reflect the higher percentage of fine-grained sediments carried in the fluvio-deltaic effluent, when compared to the Katumbi river.

The NDVI data for the watersheds demonstrate that the Katumbi watershed maintains significant vegetation cover and density in the dry season, a reflection of the

evergreen vegetation that covers the majority of the watershed (*Table 2*), whereas the Rukoma and Lagosa watersheds experience NDVI value decreases of over 60%. Although the decrease in NDVI values during the dry season for the lower elevation Rukoma and Lagosa watersheds reflects in part the semi-deciduous vegetation types which comprise most of the watershed (miombo and bamboo), part of the decrease is also related to the significant burning which takes place regularly. The NBR data demonstrates that fires occur over large areas regularly in the Rukoma and Lagosa watersheds (on average > 38 km^2) but occur at a smaller scale (on average < 5 km^2) and are more infrequent (see Hunink et al. 2015) in the Katumbi watershed (*Figure 15* and *Table 4*). Fires adjacent to Lake Tanganyika have been linked to intentional land clearance (largely for agricultural purposes), charcoal production, and uncontrolled occurrences from the usage of fire for cooking (Palacios-Fest et al. 2005). Most fires identified in our study occurred in areas identified as miombo forest or bamboo, suggesting that largely non-agricultural burning of land from charcoal production, clearing of underbrush in forested areas for small-scale cultivation of land, and unintentional occurrences from human fires are more common than those intended for clearing agricultural land.

Collectively, the remotely sensed data indicate that in comparison to the Katumbi watershed, the Rukoma and Lagosa watersheds experience more large-scale disturbance on a more frequent basis through burning, experience larger decreases in vegetation health and abundance during the dry season, and have resultant sediment plumes that are large, which is consistent with our sedimentologic data that indicates fine-grained sedimentation over a significantly larger area offshore.

Temporal Changes in Shoreline Progradation

Previous studies have observed increased progradation rates of river deltas following deforestation events within watersheds of the Ruzizi River in Lake Tanganyika (Caljon 1987) and elsewhere globally (Mattheus et al. 2009; García-Ruiz 2010). Here, the temporal changes in progradation distances of the Katumbi, Lagosa, and Rukoma rivers provide data on the nature of the fluvio-deltaic sedimentation from 1984-2016, and can perhaps be linked with discrete deforestation events and climatic fluctuations (i.e. years of drought or significant rainfall). The results indicate that the Lagosa and Rukoma rivers have prograded farther (mean distance) compared to the Katumbi river (*Figure 16*), and also show a noticeable increase in the rate of progradation between 2004 and 2007 (*Figure 11*).

The larger progradational distances of the Lagosa and Rukoma river deltas compared to the Katumbi river delta are interpreted to reflect the higher erosion rates, sediment yields, and nearshore fluvio-deltaic sedimentation attributable to increased agricultural land use, larger and more frequent burning of vegetation, and to some degree the differences in drainage area and slope. It is likely the combination of these proposed causal factors, coupled with variations in seasonal rainfall that explain the significant progradation event that occurred between 2004 and 2007 in the Rukoma and Lagosa watersheds (*Figure 11*). 2003 and 2005 were particularly dry years based on our rainfall data for the Mahale Mountains region (771 and 829 mm total rainfall), and they were both followed by years with above-average rainfall in 2004 and 2006 (1020 and 1132 mm total rainfall). In the short period between 2004 and 2007, both the Rukoma

and Lagosa river shorelines prograded approximately 40 meters, while the Katumbi prograded no significant distance over the same time period (*Figure 11*).

Because the Katumbi delta front has a steeper bathymetric gradient than the Rukoma and Lagosa delta fronts (*Figure 14*), lake-level change, which can vary significantly over short timescales (i.e. annually), was also examined as a potential explanation for the differing rates of shoreline progradation between the rivers. Lake-level regression would induce larger lakeward shoreline migration with a shallower-gradient delta front than a steeper-gradient; therefore, it is possible that the increase in shoreline progradation rate between 2004 and 2007 by the Lagosa and Rukoma rivers could be explained by lake level regression, rather than increased sediment yield and fluvio-deltaic sedimentation. Following the drought in 2003 and 2005, lake level decreased and reached minimum of ~0.5 m below the long term mean in 2006 (USDA FAS 2017). However, a change of this magnitude cannot entirely explain the ~40 m distance that the Rukoma and Lagosa shorelines prograded during the same time interval (*Figure 11*). Thus, it is interpreted that although lake level regression likely contributes to larger shoreline progradation for the shallower-gradient deltas (Rukoma and Lagosa), larger sediment yield from increased erosion following years of drought and then higher rainfall is largely responsible for the increase in shoreline progradation rate.

Impact of Land-Use Change on Nearshore Sedimentation

Previous studies have demonstrated that many rivers globally have seen dramatic increases in sediment flux from intensive agriculture and deforestation in recent decades (e.g. Walling and Fang, 2003), and particularly the effect that land-use

change has on fine-grained sedimentation in lacustrine environments (e.g. Cisternas et al. 2001; Walling et al. 2003; Donohue et al. 2003; Donohue and Molinos 2009). Bizimana and Duchafour (1991) examined erosion rates for watersheds at the northern end of the lake in Burundi, and found, for deforested and cultivated lands, erosion rates up to 100 tons/ha/yr, largely due to rapid headward erosion, stream incision, and gully formation that occurs following rapid deforestation (Cohen et al. 1993b). Nkotagu and Mbwambo (1999) completed a study in Lake Tanganyika (northern Tanzanian coastline) that compared a protected watershed to one that was largely colonized and cultivated for agriculture, and found that the altered watershed had a suspended sediment load an order of magnitude greater relative to the protected watershed. The suspended sediment from the impacted watershed was also finer-grained, with significant clay minerals. Overall, previous studies, focused mostly on rocky shorelines in Lake Tanganyika, have identified coupled deforestation and rapid erosion as the most severe environmental problems that threaten Lake Tanganyika (Nsabimana 1991; Cohen et al. 1996).

In the Mahale Mountains region, deforestation and burning within a watershed would likely result in a higher proportion of fine-grained sediment erosion and entrainment into fluvial systems, given that they are more abundant in well-developed soils exposed at the surface and are highly erodible following the removal of vegetation. This phenomenon is observed in the grain size, mud size, and % clay data offshore of the Rukoma and Lagosa watersheds, where larger swaths of land are subject to burning and agricultural land-use resulting in more fine-grained sediments, with a higher percentage of clay compared to the Katumbi watershed (*Tables 2 and 4*), (*Figures 15*

and 17). The PCA results also show that the sediments offshore of the Katumbi watershed are a distinguished statistically compared to those offshore of the Rukoma and Lagosa watersheds.

These differences could be explained by the primary sediment creation mechanisms that exist within the watersheds, since the underlying bedrock geology is constant throughout the area's watersheds (Paleoproterozoic gneiss, granulite, migmatite, amphibolite, and quartzite; Kabete et al. 2012). In the Katumbi watershed, high relief slopes exposing the Precambrian metamorphic rocks result in the production of coarse sand and gravel rather than clay, with little disturbance of well-developed soil horizons. However, in the Rukoma and Lagosa watersheds, where there is widespread burning of native miombo forest and herbaceous vegetation, deeply weathered oxisol soils are easily eroded generating large volumes of largely fine-grained sediment that are clay-rich (*Figure 17*), a phenomenon recognized in humid tropical regions (Obi et al. 1989). Additionally, the vegetation which typically replaces burned or cultivated land following native vegetation removal are typically grasses or an agricultural vegetation type (typically cassava and maize in the Mahale region), which are less effective at maintaining soil integrity and preventing erosion when the wet season precipitation begins inundating the region in late September (Bizimana and Duchafour 1991).

Differences in slope, watershed size, and discharge can also result in sediment loads that are coarser or finer. Specifically, steeper, smaller watersheds tend to have sediment loads that are coarser, whereas larger watersheds with shallower gradients and larger floodplains tend to have muddier sediment loads (Orton and Reading 1993).

Therefore, in our study it is important to separate the effect that differences in physical characteristics of watersheds will have on sediment texture from the effect that disturbance of soils rich in fine-grained clastic material will have on the sediment textures derived from each watershed. The Katumbi watershed is steeper and smaller than the Lagosa and Rukoma watersheds (*Table 1*). Although this could result in the Katumbi river carrying a naturally coarser sediment load, other studies have noted that steeper watersheds generally have much higher erosion rates (Montgomery and Brandon 2002), which can be exacerbated by vegetation removal along high-relief hillslopes. In such cases, large amounts of fine-grained clay-rich sediment from disturbed soils would also be carried with the generally coarser bedload. Because the Katumbi watershed is largely unaffected by deforestation and agricultural land use, the coarser sediment load is interpreted to reflect the lack of soil horizon disturbance, resulting in a lack of fine-grained clay-rich sediment offshore. Similarly, the finer sediment load carried by the Lagosa and Rukoma rivers, which have watersheds with more agricultural land-use and deforestation from burning, can be attributed mostly to the disturbance of clay-rich soils, rather than the tendency of rivers with larger watersheds and shallower gradients to carry a finer sediment load.

Hunink et al. (2015) identified a strong correlation between the fire return interval and the modeled sediment yield for the same watersheds as this study in the Mahale Mountains. The study found that the Lagosa and Rukoma watersheds have more frequent fires, and their maximum annual specific sediment yield (21 and 14 ton/ha/yr, respectively) exceeds that of the Katumbi watershed (12 ton/ha/yr). The study also concluded that fires have more frequent return intervals and specific sediment

yields in herbaceous (3 yr, 6 ton/ha/yr), miombo (4 yr, 3 ton/ha/yr), bamboo (3 yr, 12 ton/ha/yr), and non-converted agricultural (4 yr, 33 ton/ha/yr) land cover types compared to evergreen forest (8 yr, 3 ton/ha/yr). The Katumbi watershed is primarily composed of evergreen forest that burns infrequently, whereas the Lagosa and Katumbi watersheds have land cover types prone to more frequent burning that also produce a higher sediment yield (miombo, bamboo, herbaceous, and agricultural land cover). Importantly, the land cover type that often is created after burning occurs is bare land, which has the highest specific sediment yield computed in the study (36 ton/ha/yr) (Hunink et al. 2015).

The relationship between land cover type, fire return interval, and specific sediment yield is likely exacerbated by the monsoonal variation of climate, where the wet season is characterized by more drastic deluges of rain immediately following the dry season when the large-scale burning takes place (Drake et al. 1999; Donohue et al. 2003; Cohen et al. 2005; Hunink et al. 2015). This pattern has been noted by previous studies, which suggest that monsoonal variations in rainfall result in higher sediment yields (Drake et al. 1999; Nkotagu and Mbwambo 1999; Patterson 2000), and thus watersheds where rapid environmental change has occurred, such as the Rukoma and Lagosa watersheds, are particularly susceptible to significant denudation.

The collective results of the study suggest that the burning of large swaths of land during the dry season, the absence of native evergreen forest vegetation in altered watersheds, and short, rapid rainfall events in the wet season are responsible for the differences in grain sizes and mud fraction size distribution observed between the sediments found offshore of the largely unaffected Katumbi river watershed and the

Lagosa and Rukoma river watersheds. These conclusions underscore the significant risk that exists within many larger watersheds in Lake Tanganyika, where widespread deforestation or cultivation of agricultural crops not well suited for preventing erosion result in land cover which is particularly susceptible to erosion and can lead to significant increases in fine-grained sedimentation and delta shoreline progradation. Other researchers (Cohen et al. 1993b; Cohen et al. 2005) have noted that it is the larger watersheds that pose the largest threat to the littoral ecosystem in Lake Tanganyika through increased sedimentation of fine-grained sediment, and our study strongly supports that notion.

Impact of Sediment Texture and Substrate Composition on the Benthic Ecosystem

The use of benthic ecological metrics such as ostracode abundances and diversity as a proxy for benthic community health has provided past evidence of the decreased abundance and diversity in response to changes in sedimentation from onshore disturbance (Cohen et al. 1993b; Alin et al. 1999; Cohen et al. 2005). Here, the results from the sponge abundance data reveal that in areas where sponges are most abundant, shell-bed substrate is also dominant and mud content is low; however, where mud content is high adjacent to the river mouths, sponges are largely absent.

These results may be indicative of the requirement for littoral sponges to attach themselves to a hard substrate that exists uniquely in shell beds unaffected by recent sedimentation observed elsewhere in the lake and in other lacustrine environments (Manconi and Pronzato 2008; Soreghan 2016). The amount of mud and presence or absence of shell-bed substrate present themselves as controlling factors for the abundance of littoral sponges in the study area, and perhaps can be extrapolated as a

proxy for overall benthic level aquatic species health. Although benthic aquatic species respond differently to increased sedimentation (e.g. Donohue and Molinos 2009), observations from the field in our study (pers. obs. 2015) and previous studies (Soreghan et al. 2016) note that fish nests constructed using shells decrease with increased clastic sedimentation in Lake Tanganyika. Previous studies have also noted that shells are a resource utilized by certain fish species, and become a source of competition when scarce (Coulter 1991; Sato 1994; Rossiter 1995; Bills 1996). Thus, with decreased shell density due to an influx in clastic sedimentation, there are generally less fish due to increased competition for shells used to construct nests for brooding.

Furthermore, studies of cichlid fish species in other African Great Lakes have found evidence that increased sedimentation imposes a largely negative impact on species abundance and diversity (Maruyama et al. 2010 and references therein). Thus, in areas where shell material has been significantly inundated by largely fine-grained fluvio-deltaic sediment in our study area, it can be extrapolated that not only the abundance of sponges, but certain fish species that use the shells to nest and are also likely affected, but this should be tested with studies focused on species abundance and health.

In 2015 and 2016, our research team recovered live *N. tanganyicense* specimens, the shells of which dominate the shell beds, between 12 and 20 m water depth inhabiting a shallow delta front environment consisting of coarse sand to silt adjacent to the Katumbi river (*Figure 14*). We also observed significant terrestrial organic matter and underwater vegetation where the live snails lived. In contrast to the two other

fluvio-deltaic systems studied in the Mahale Mountains region, the sediments collected from the lake floor were generally coarser, the water was less turbid, and there was more terrestrial organic matter and aquatic vegetation in the delta where the live snails were observed. Also, the Katumbi watershed is relatively unaltered compared to those elsewhere in the lake, where widespread burning and agricultural land-use have removed native vegetation cover (*Table 2 and Figure 15*).

Given the importance of the Katumbi delta as a potential refugia for a small population of *N. tanganyicense* snails, a more directed effort was implemented in 2016 for examining the area and collecting shell samples. Preliminary observations of the taphonomy of the shell beds adjacent to the Katumbi river delta suggest that they are composed of largely unfragmented, unencrusted, pristine, *N. tanganyicense* shells. By comparison, the shell beds not yet covered by fluvio-deltaic sediments adjacent to the Rukoma and Lagosa rivers are composed largely of encrusted, *N. tanganyicense* and *Coelatura sp.* shells. Given that the only live specimens observed during field work were adjacent to the Katumbi river delta, it is interpreted that the shell beds fringing the Katumbi delta shell beds could represent young, very recent accumulations sourced by a remnant population of live *N. tanganyicense*. Further work using geochronological methods and taphonomical analyses is required to test the validity of this.

Although preliminary, these observations are important in our understanding of the life history and cause of mortality of one of the most important shell-bed constituent species in Lake Tanganayika, *N. tanganyicense*. It seems that the interpretation that adult *N. tanganyicense* snails rely largely on filter feeding of particulate organic matter while buried in a coarse substrate (West et al., 1991; pers. obs. 2015) is at odds with

previous interpretations that *Neothauma sp.* snails are exclusively mobile and actively prey on endobenthic organisms (Van Damme and Pickford 1999). However, if our observations are valid, the modern absence of *N. tanganyicense* in the field area is consistent with the sediment texture differences among the deltas. Filter feeding by gastropods would be particularly susceptible to increased turbidity (Donohue and Irvine 2004).

A core taken by Cohen et al. (2005) within the Mahale Mountains study area (*Figure 3*) revealed that more moderate land-use change and incipient increased sedimentation has occurred within the region since the 1960's, but the area has not experienced the magnitude of change which has impacted watersheds farther north. The Katumbi river delta and its live *N. tanganyicense* population could perhaps provide a glimpse into the habitat of the snails prior to the large-scale colonization and subsequent alteration that has occurred adjacent to Lake Tanganyika since the late 18th and early 19th centuries (Alin et al. 2002; Cohen et al. 2005; Palacios-Fest et al. 2005; Kashaigilia and Majaliwa 2013; Conaway et al. 2012; Odigie et al. 2014).

Conclusions

The nearshore environment of Lake Tanganyika serves as a nursery to one of the most diverse populations of endemic aquatic fauna in the world, which are an essential resource to its growing coastal communities. This study is the first within Lake Tanganyika to combine remote sensing and sedimentologic techniques to examine the intimate relationship between onshore watershed disturbance, the sedimentology of the littoral environment, and the benthic organisms which live there. Results from this study indicate that increased watershed disturbance in the form of widespread burning of land and agricultural land-use correlate with decreases in overall grain size, increased sediment clay content, increases in shoreline progradation distance, increased fluvio-deltaic sediment plume size, and decreased abundance of littoral sponges. Importantly, our study suggests that the occurrence of the poorly understood, but crucial component of the shell beds in Lake Tanganyika, *Neothauma tanganyicense*, is tied to the onshore watershed disturbances.

In agreement with previous studies, we suggest that the influx of fine-grained clastic sediments into the littoral environment following widespread vegetation removal and soil erosion poses a significant threat to the nearshore ecosystem. Furthermore, we identify the relatively unaffected Katumbi watershed as a potential modern-day refugia for a small surviving population of *N. tanganyicense*, and perhaps could provide an example of what many watersheds in Lake Tanganyika were like prior to the large-scale colonization and subsequent deforestation of the nearshore environment and hinterland of the lake that has occurred since the late 18th and early 19th centuries. Future conservation efforts aimed at mitigating such deleterious effects from inundating the

nearshore environment elsewhere in the lake should include wildfire prevention, expanding riparian buffers adjacent to fluvial systems, and implementation of agricultural best practices for preventing soil erosion in at-risk areas.

Figures

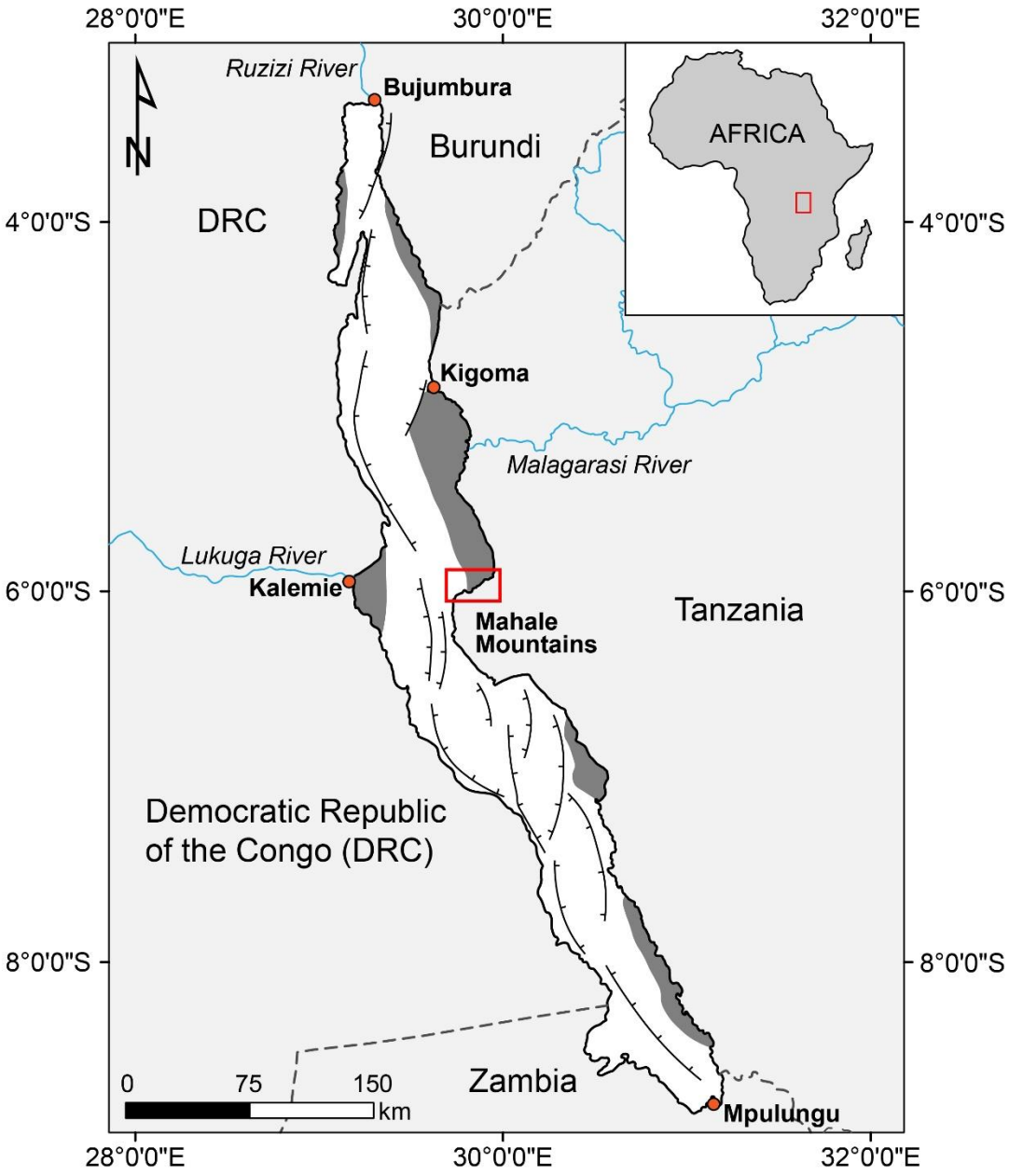

Figure 1 Location of Lake Tanganyika in Africa (inset) and its major structural elements. Hinged littoral platforms are shaded dark grey. Red box indicates Mahale Mountains study area. Modified from McGlue et al. (2010).

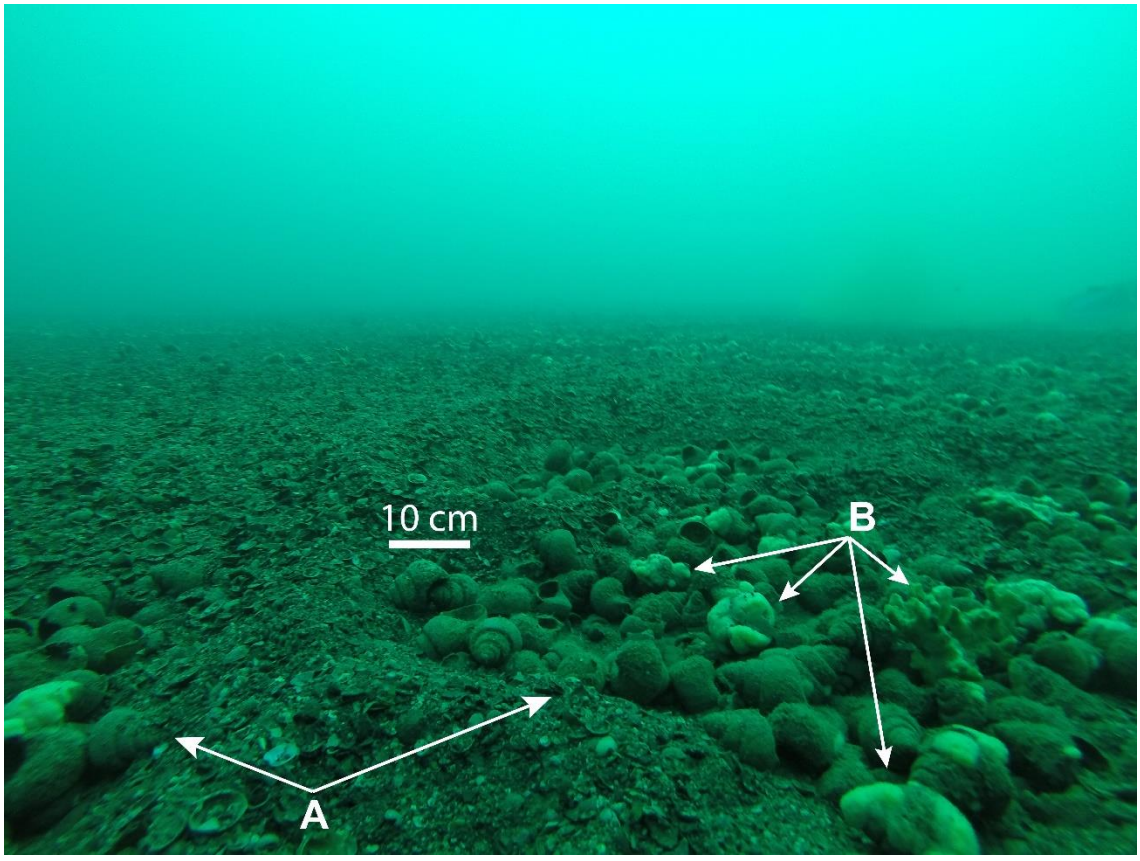

Figure 2 Representative picture of the shell-bed habitat in the Mahale Mountains study area. The clusters of larger *N. tanganyicense* shells on the right and left sides of the picture are fish nests (A), and light colored branching morphs attached to shells are sponges (B) (photo taken at 20 m depth along T6).

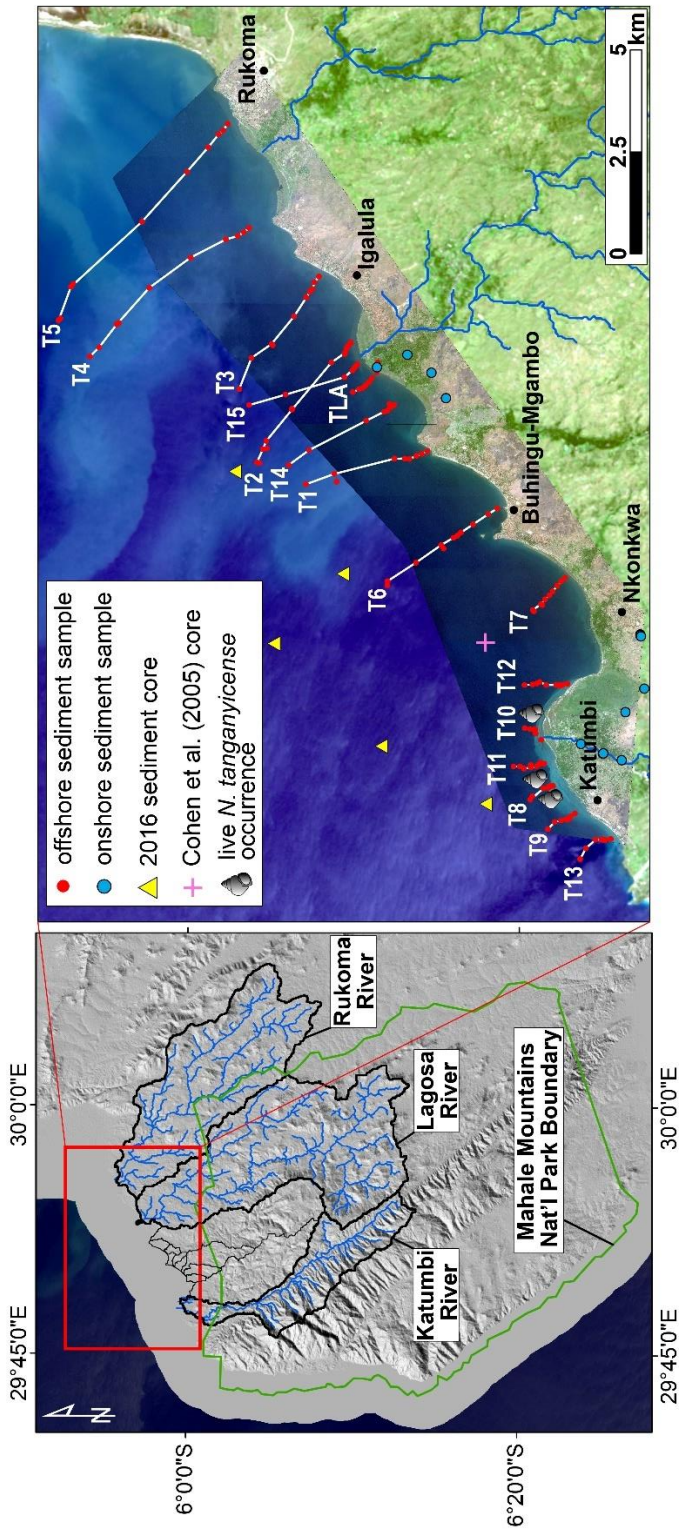

Figure 3 Study area location within the Mahale Mountains National Park area (left) of western Tanzania. Red box shows location of image on right that displays the sampling transects, rivers, and population centers within the study area. Proprietary imagery courtesy of the DigitalGlobe Foundation.

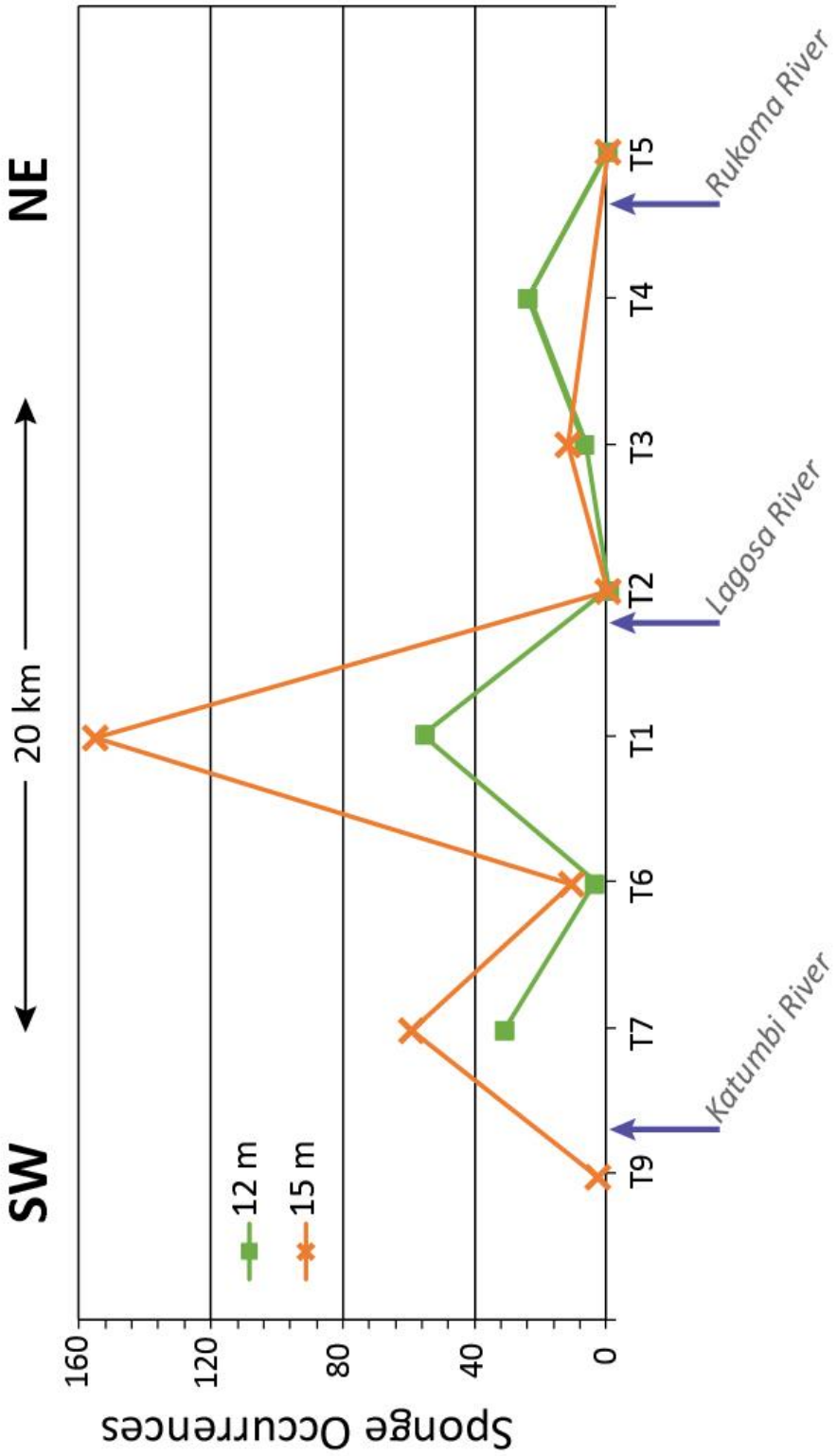

Figure 4 Sponge occurrences at 12 and 15 m water depth.

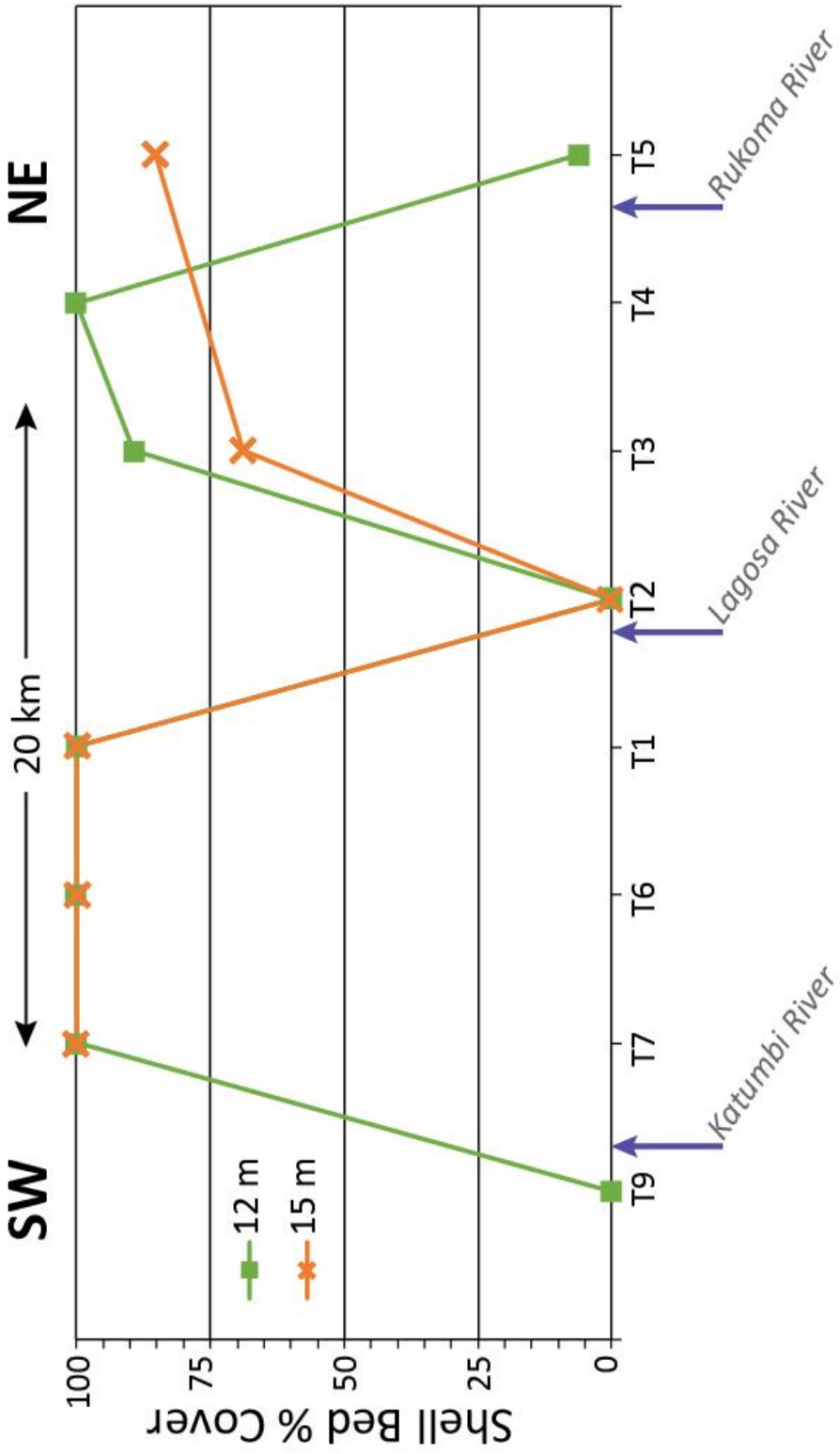

Figure 5 Shell bed % cover at 12 and 15 m water depth

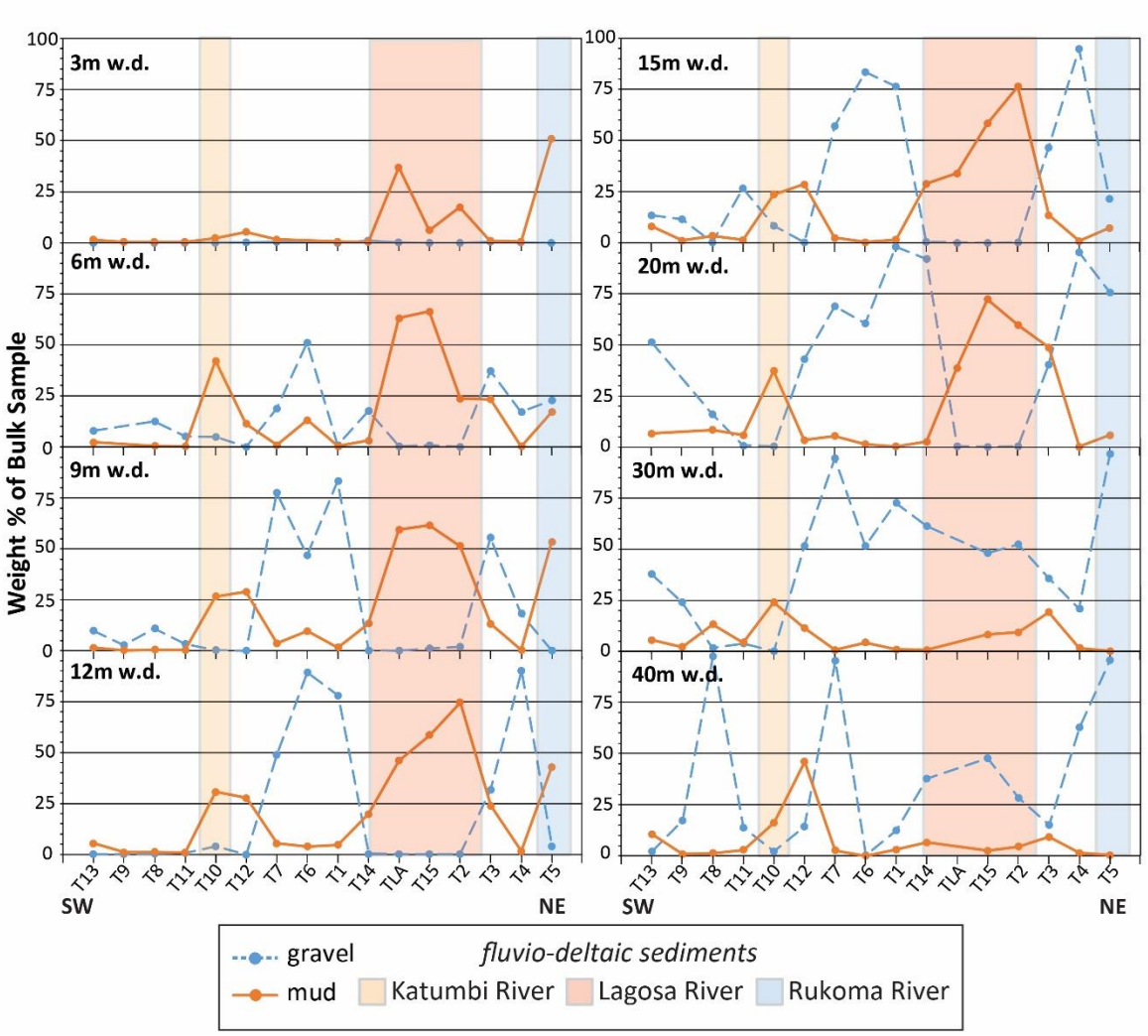

Figure 6 Grain size weight % for 3-40 m water depth

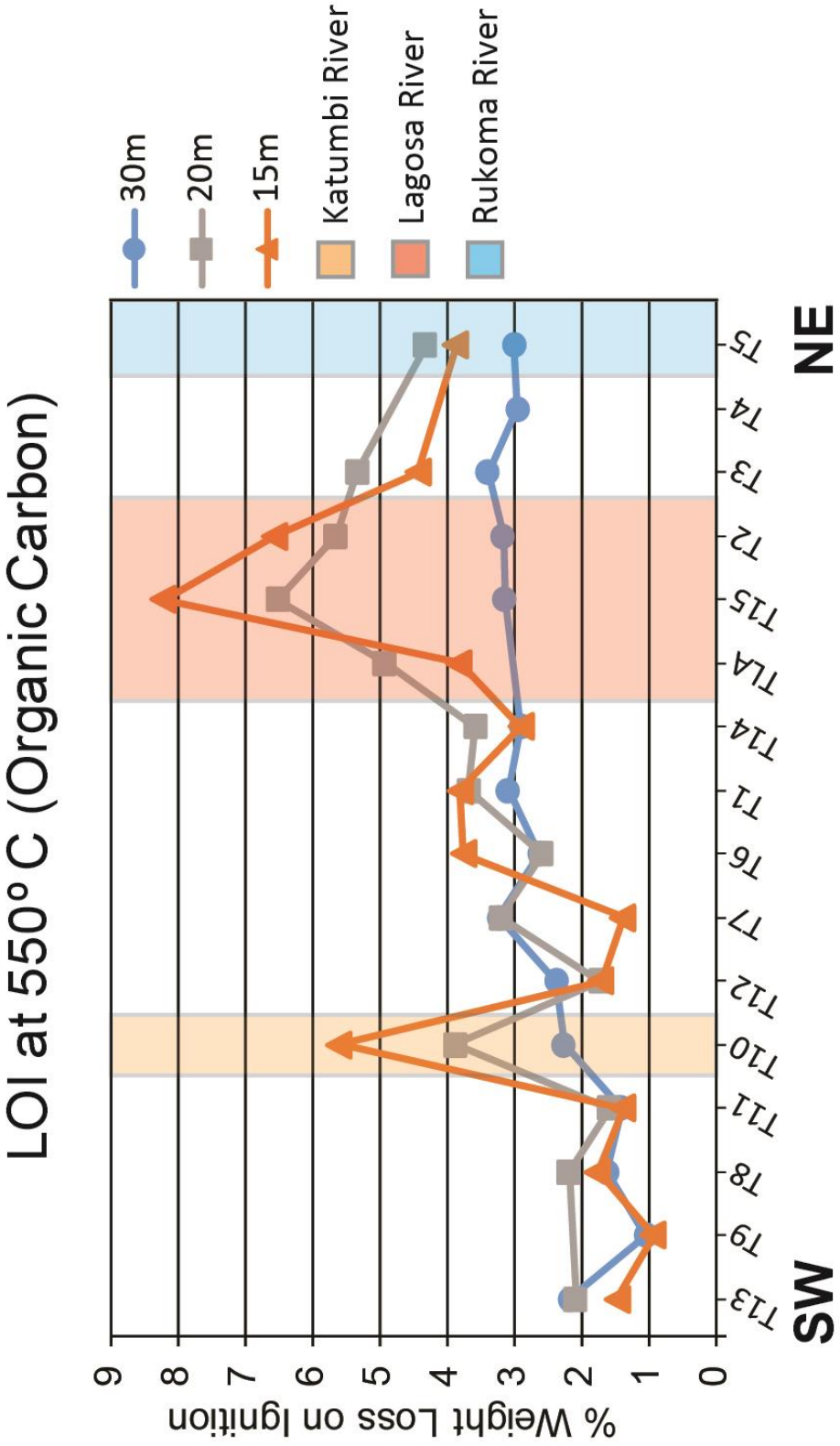

Figure 7 Loss on Ignition (LOI) values at 550° C for 15, 20, and 30 m water depth.

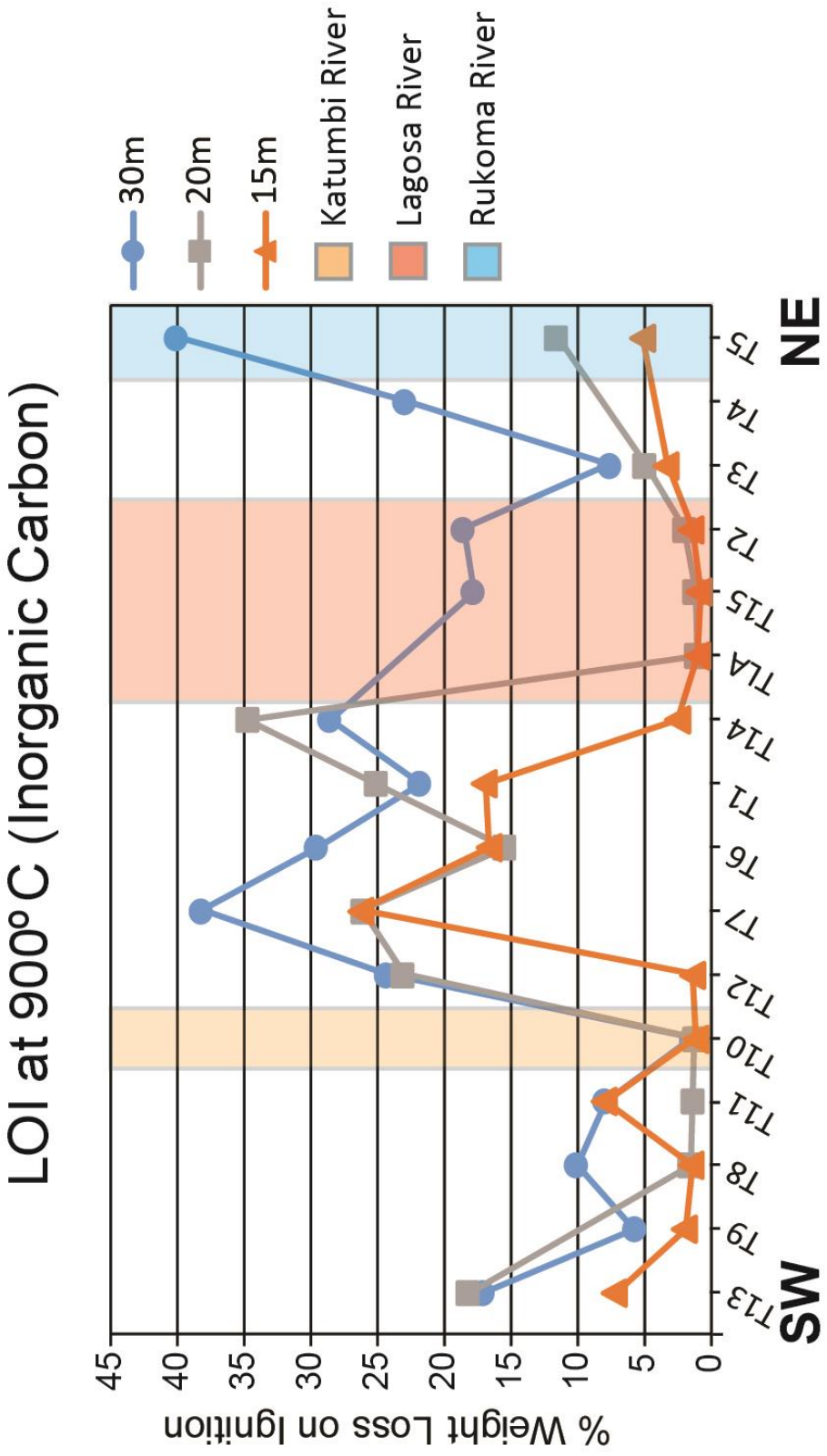

Figure 8 Loss on Ignition (LOI) values at 900º C for 15, 20, and 30 m water depth.

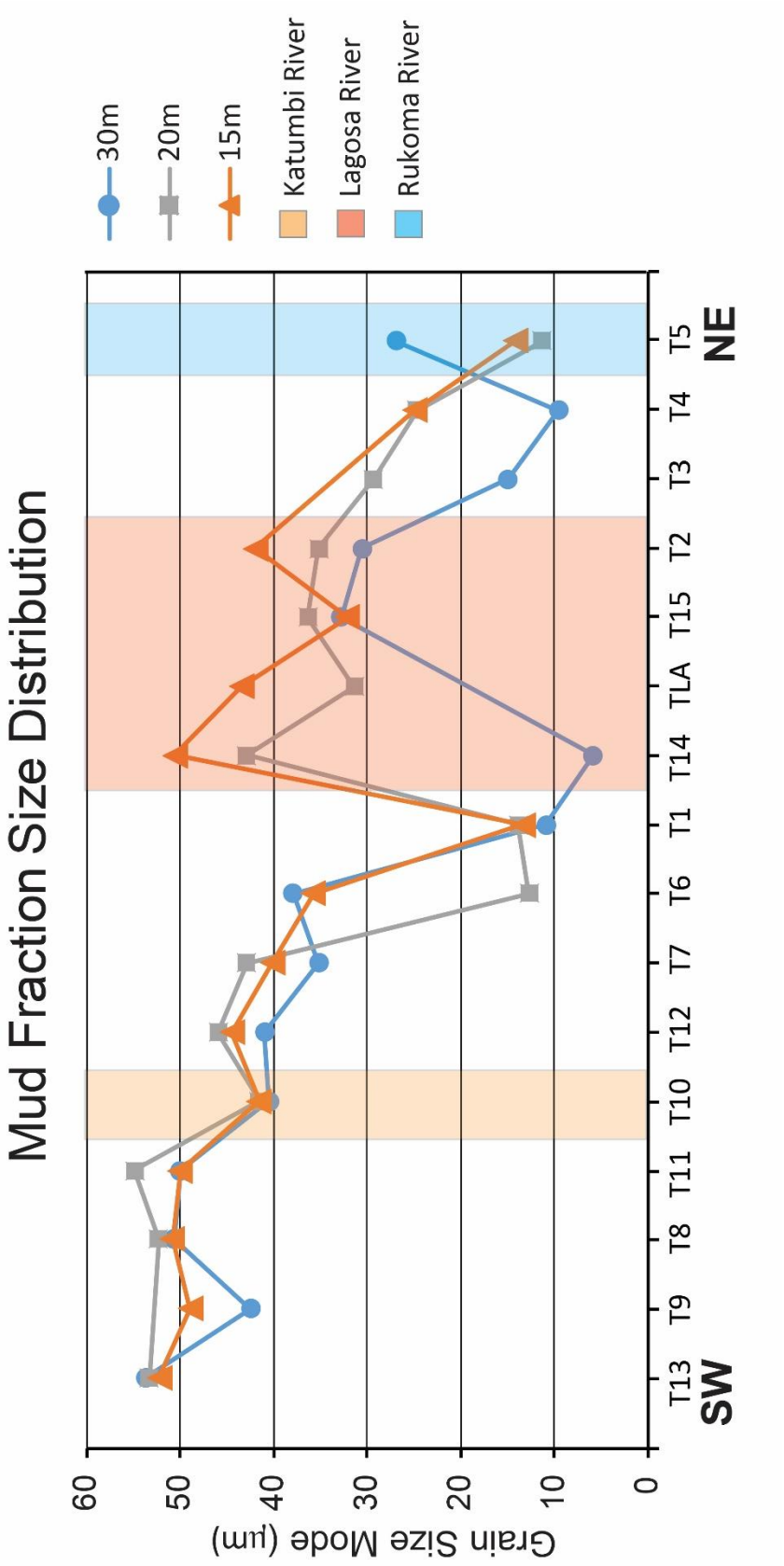

Figure 9 Grain size mode of the mud fraction of the bulk sediment samples.

Figure 10 Examples of the size of sediment plumes from the Katumbi, Lagosa, and Rukoma river deltas (Landsat 5 image captured 10/30/1991).

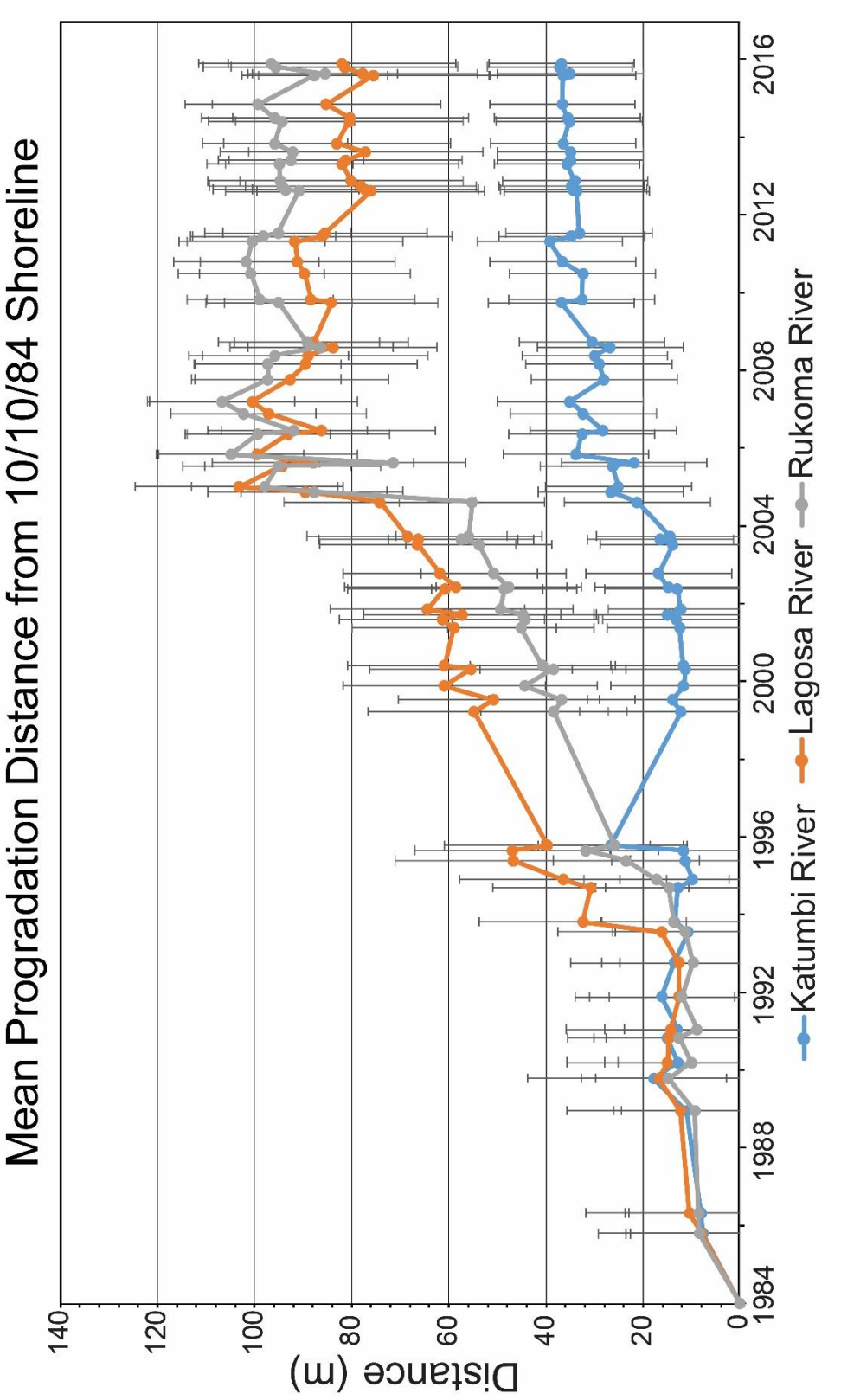

Figure 11 Temporal change in the mean yearly progradation distance from the 1984 shoreline.

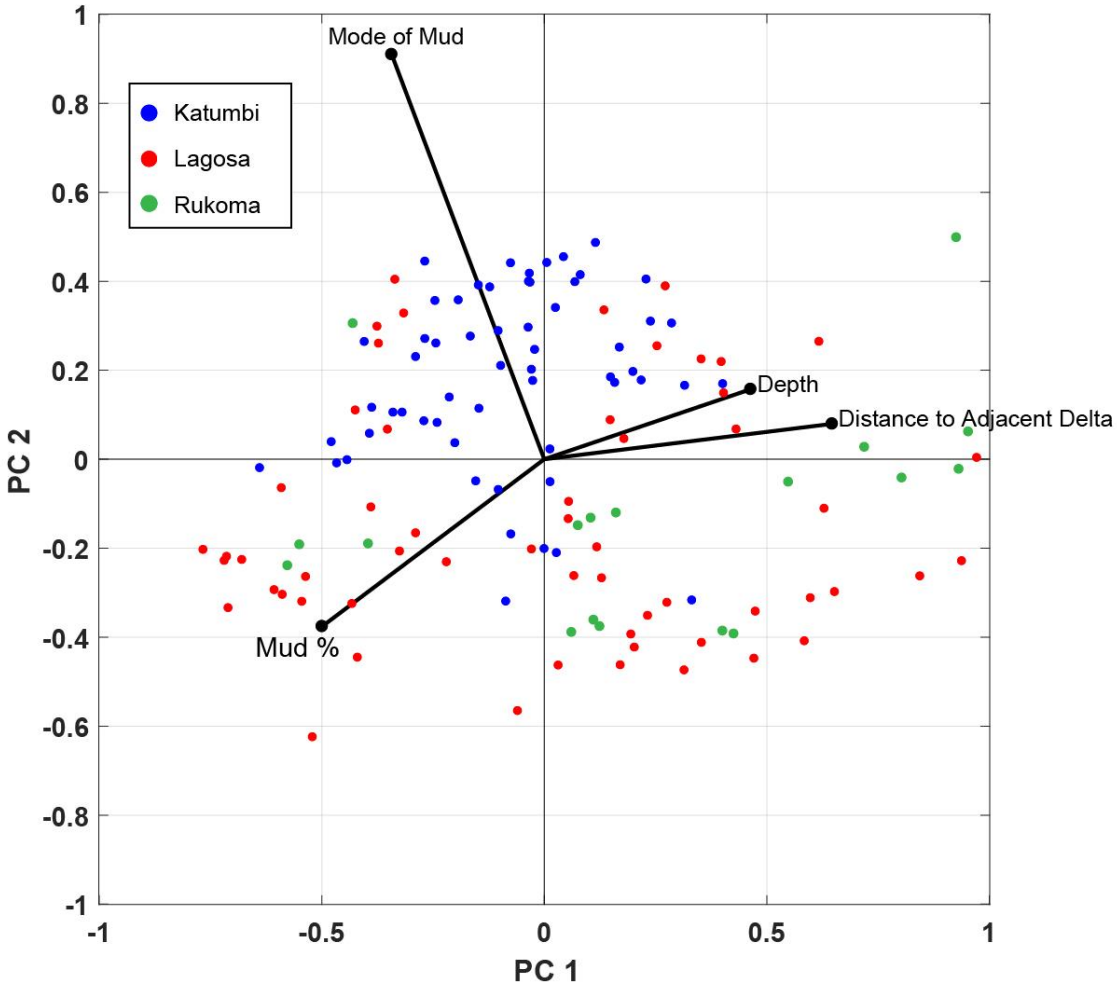

Figure 12 Principal component analysis results as a biplot of PC1 and PC2 with projected variable loadings as vectors from the origin and samples coded by their proximity to the three river mouths.

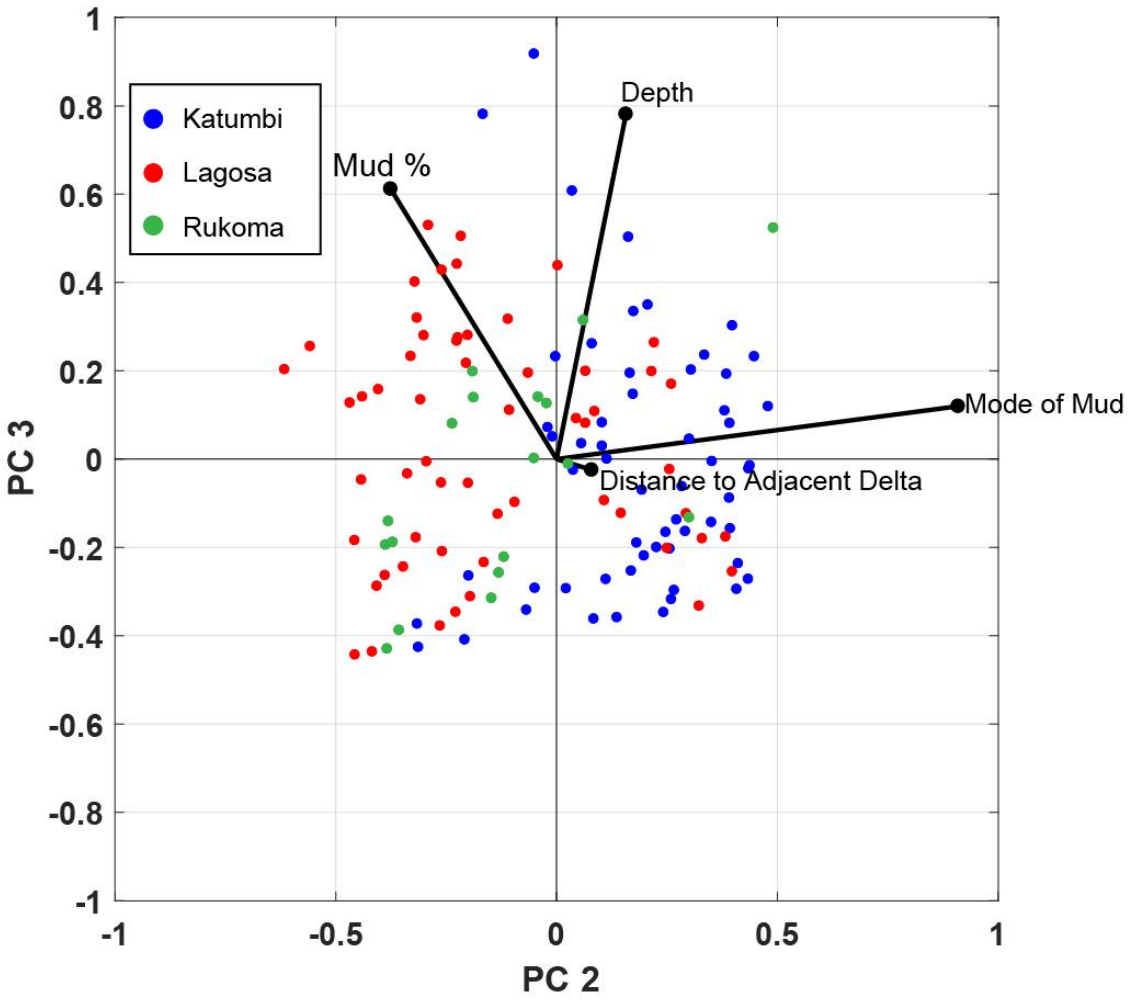

Figure 13 Principal component analysis results as a biplot of PC2 and PC3 with projected variable loadings as vectors from the origin and samples coded by their proximity to the three river mouths.

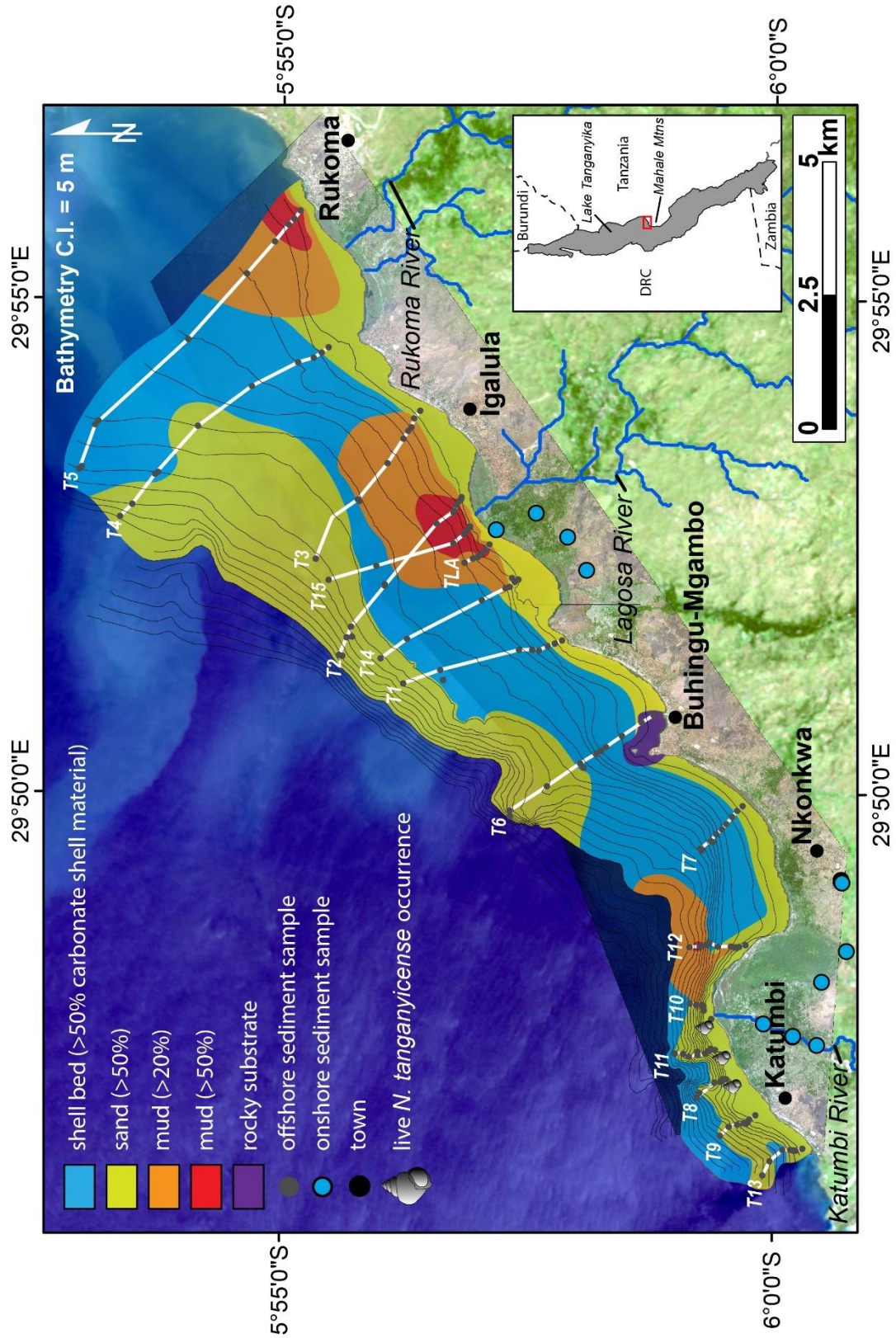

Figure 14 Facies map of the Mahale Mountains study area based on data from this study. Proprietary satellite imagery courtesy of the DigitalGlobe Foundation.

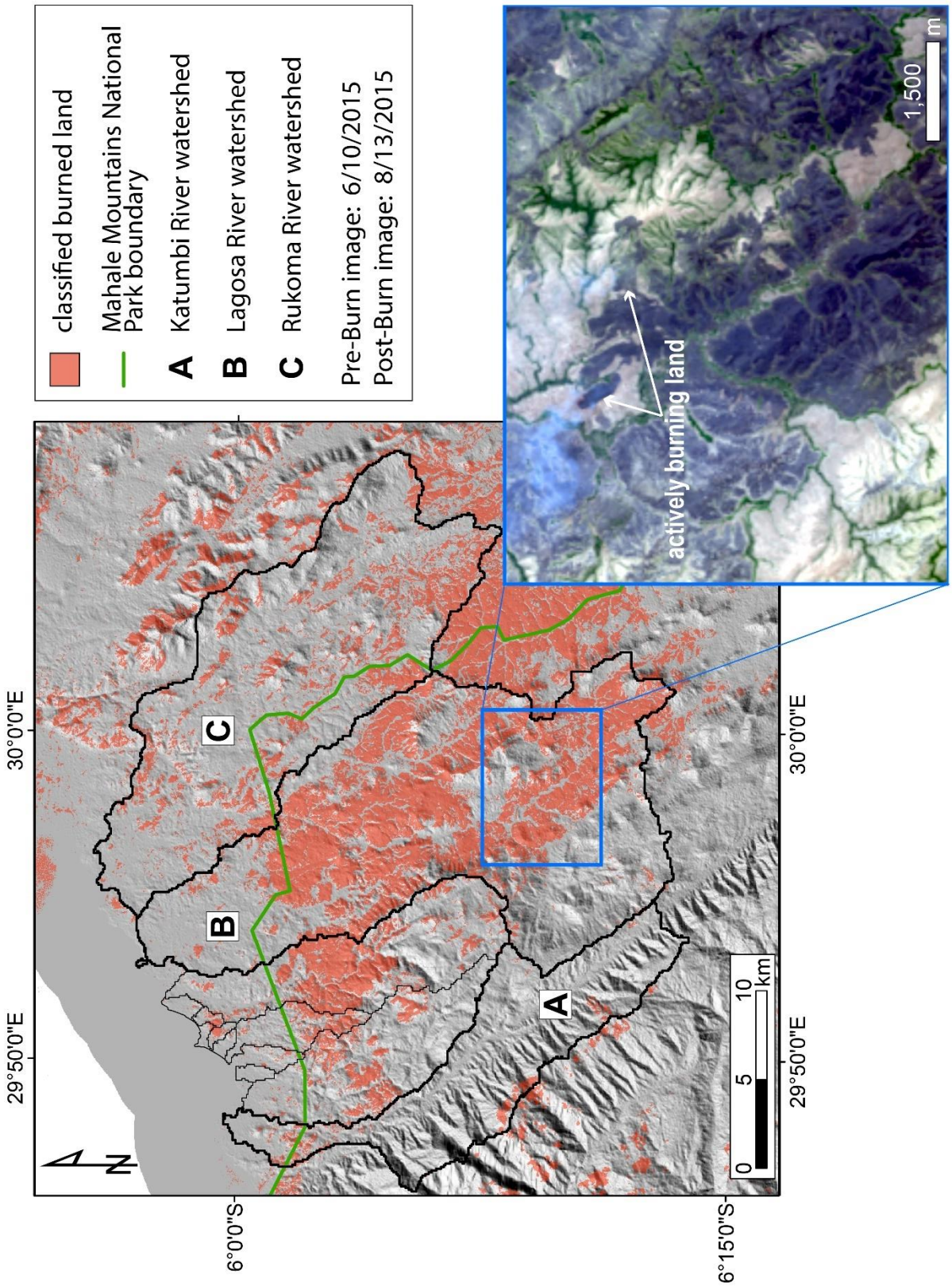

Figure 15 Example of the burned area calculation for the study area's watersheds based on the normalized burn ratio (NBR) computed for images from 6/10/15 and 8/13/15.

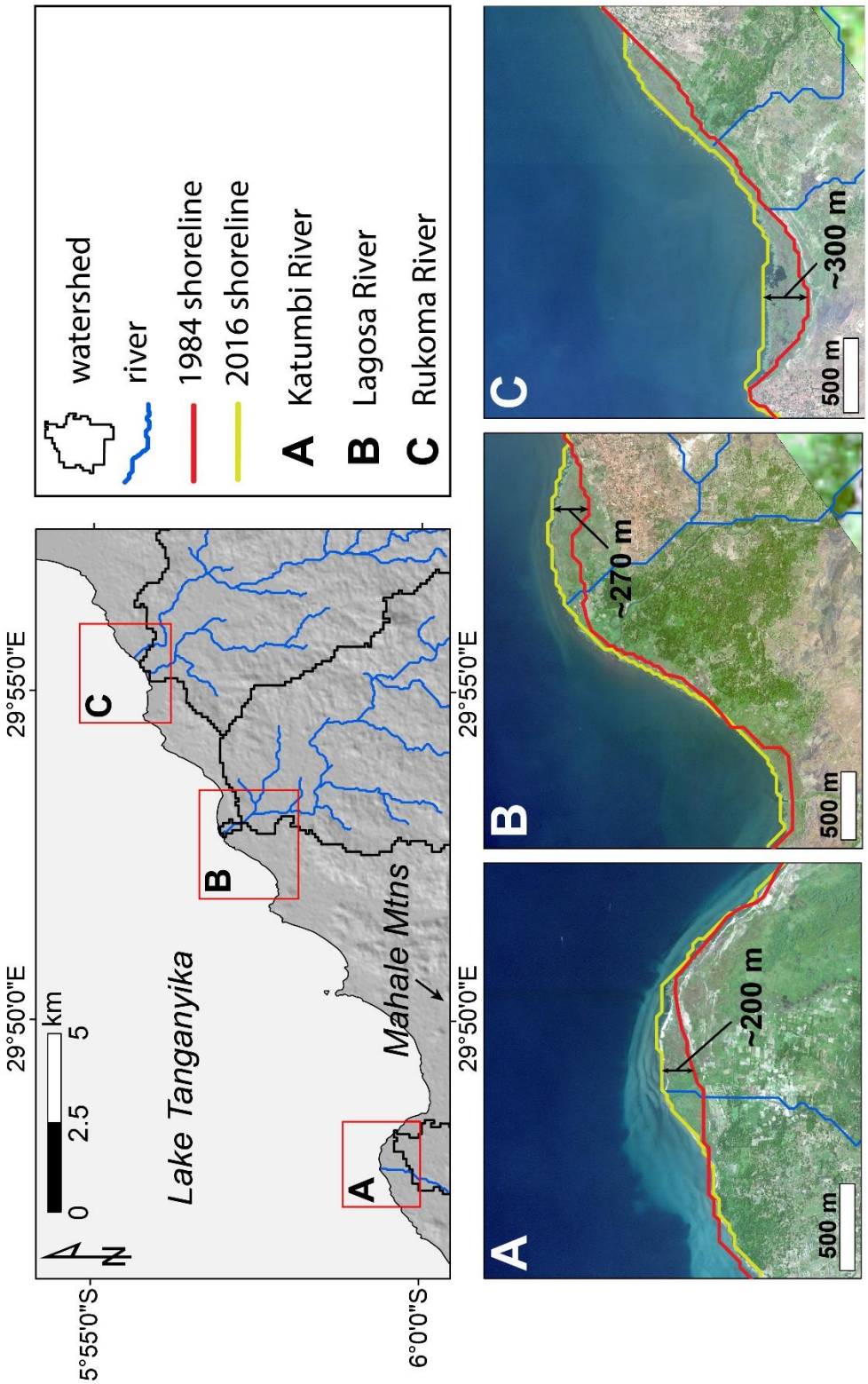

Figure 16 Cumulative progradation distances for the interval 1984-2016 for the Katumbi, Lagosa, and Rukoma river deltas. Proprietary imagery courtesy of the DigitalGlobe Foundation.

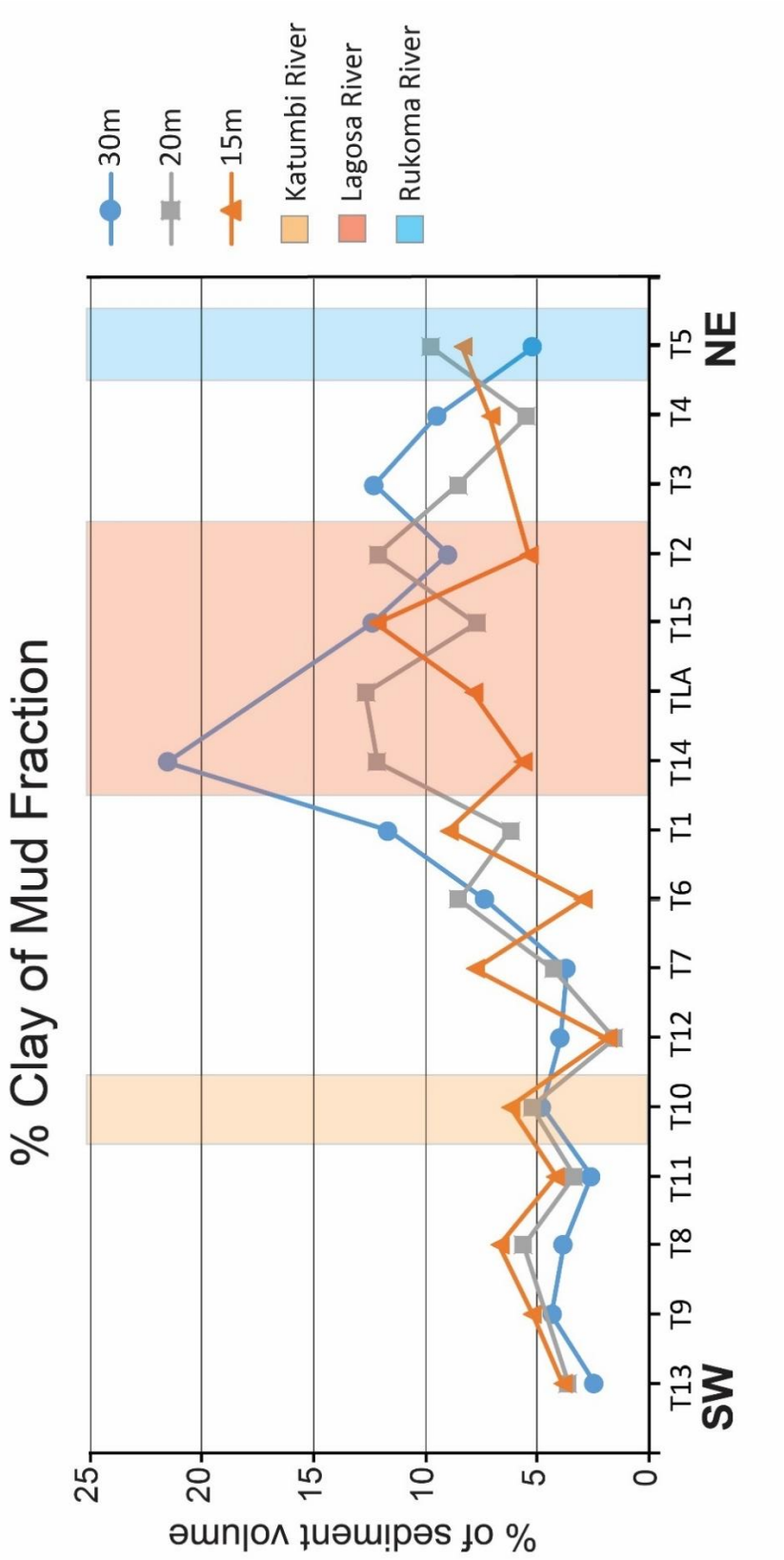

Figure 17 Volume percent clay (< 3.9 μm) of the mud fraction of the bulk sediment samples.

Tables

	Katumbi	Lagosa	Rukoma
Size (km^2)	112	314	242
Avg Elevation (m)	1549	1164	1118
Max Elevation (m)	2501	1905	1878
Avg Slope (degrees)	19	10	8
Max Slope (degrees)	62	56	59

Table 1 Summary of physical attributes for three largest watersheds in the study area

Table 2 Summary of land cover types (2001-2014) for the study area watersheds

	Katumbi		Lagosa		Rukoma	
Land Cover	Area (km^2)	% of watershed area	Area (km^2)	% of watershed area	Area (km^2)	% of watershed area
rice	0.3	0.3%	0.0	0.0%	0.4	0.2%
bamboo	6.4	5.7%	122.3	38.9%	75.5	31.2%
mixed agriculture	8.1	7.3%	25.9	8.3%	20.7	8.5%
palm	0.4	0.4%	2.6	0.8%	2.7	1.1%
evergreen forest	48.4	43.4%	10.9	3.5%	16.9	7.0%
miombo	24.3	21.8%	125.7	40.0%	104.3	43.1%
residential	0.0	0.0%	0.4	0.1%	0.2	0.1%
herbaceous	22.9	20.5%	23.9	7.6%	9.4	3.9%
forest loss	0.2	0.2%	2.3	0.7%	11.8	4.9%

Year	Annual Total Rainfall (mm)
2015	1031
2014	1052
2013	1060
2012	1029
2011	1109
2010	869
2009	1129
2008	1004
2007	914
2006	1132
2005	829
2004	1020
2003	771
2002	1026
2001	886
Mean Annual Rainfall = 991	
Standard Deviation = 108	

Table 3 Annual rainfall totals for the Mahale Mountains region, Tanzania

Pre-Burn Image Date	Post-Burn Image Date	Sensor	NBR Burned Land Class Values	Total Area Burned (km^2)		
				Katumbi	Rukoma	Lagosa
5/11/2016	8/31/2016	Landsat 8	0.65 - 1.61	4.8	89.1	30.5
6/10/2015	8/13/2015	Landsat 8	0.47 - 1.22	4.7	124.5	44.8
5/22/2014	8/10/2014	Landsat 8	0.56 - 1.53	7.5	40.8	63.4
5/19/2013	8/23/2013	Landsat 8	0.58 - 1.45	6.2	58.2	42.7
5/13/2002	8/17/2002	Landsat 7	0.44 - 1.37	1.3	40.3	53.4
5/5/2008	8/9/2008	Landsat 5	0.36 - 1.30	1.3	17.2	24.0
6/14/2005	9/2/2005	Landsat 5	0.28 - 1.32	2.8	25.9	24.3
6/19/1995	9/7/1995	Landsat 5	0.44 - 1.49	6.9	39.2	18.3

Table 4 Summary of watershed normalized burn ratio (NBR) computations

Eigenvectors	Eigenvalue	Variance Explained (%)	Cumulative Variance (%)
PC1	1.80	45.0	45.0
PC2	0.92	22.9	67.9
PC3	0.86	21.6	89.5
PC4	0.42	10.5	100.0

Table 5 Contribution of each eigenvector to the observed variance

	PC1	PC2	PC3	PC4
Distance to Adjacent Delta	**0.647**	0.080	-0.025	**0.758**
Depth	**0.464**	0.157	**0.781**	-0.387
Mud %	**-0.499**	-0.376	**0.612**	**0.485**
Mode of Mud	-0.343	**0.910**	0.120	0.201

Table 6 Summary of loading values of the variables for each of the principal components. The most important variables are highlighted.

References

Abdi H, Williams LJ (2010) Normalizing data. In: Salkind NJ, Dougherty DM, Frey B (eds.) Encyclopedia of Research Design. Thousand Oaks, California.

Alin SR, Cohen AS, Bills R, Gashigaza MM, Michel E, Tiercelin JJ, Martens K, Coeveliers P, Mboko SK, West K, Soreghan MJ, Kimbadi S, Ntakimazi G (1999) Effects of landscape disturbance on animal communities in Lake Tanganyika, East Africa. Conserv Biol 13:1017–1033. doi:10.1046/j.1523-1739.1999.96476.x

Alin SR, O'Reilly CM, Cohen AS, Dettman DL, Palacios-Fest MR, McKee BA (2002) Effects of land-use change on aquatic biodiversity: A view from the paleorecord at Lake Tanganyika, East Africa. Geol 30:1143–1146

Bills RI (1996) Eco-ethology of shell dwelling Cichlids in Lake Tanganyika. Unpublished M.Sc thesis, Rhodes University, Grahamstown, South Africa. pp 1–47

Bizimana M, Duchafour H (1991) A drainage basin management study: The case of the Ntihangwa River Basin. In: Cohen A.S. (ed.), Report of the first international conference on conservation and biodiversity of Lake Tanganyika. Biodiversity Support Program, Washington, DC, pp. 43–45

Caljon AG (1987) A recently landlocked brackish-water lagoon of Lake Tanganyika: physical and chemical characteristics, and spatio-temporal distribution of phytoplankton. Hydrobiologia 153:55–70. doi: 10.1007/bf00005504

Casanova J, Hillaire-Marcel C (1992) Late Holocene hydrological history of Lake Tanganyika, East Africa, from isotopic data on fossil stromatolites. Palaeogeogr Palaeoclimatol Palaeoecol 91:35–48

Cisternas M, Araneda A, Martínez P, Pérez, S (2001) Effects of historical land use on sediment yield from a lacustrine watershed in central Chile. Earth Surf Processes and Landf 26:63–76. doi: 10.1002/1096-9837(200101)26:1<63::aid-esp157>3.0.co;2-j

Cohen AS, Thouin C (1987) Nearshore carbonate deposits in Lake Tanganyika. Geology 15:414. doi: 10.1130/0091-7613(1987)15<414:ncdilt>2.0.co;2

Cohen AS (1989a) The taphonomy of gastropod shell accumulations in large lakes: An example from Lake Tanganyika, Africa. Paleobiology 15: 26-45

Cohen AS (1989b) Facies relationships and sedimentation in large rift lakes and implications for hydrocarbon exploration: Examples from lakes Turkana and Tanganyika. Palaeogeogr Palaeoclimatol Palaeoecol 70:65–80. doi: 10.1016/0031-0182(89)90080-1

Cohen AS, Soreghan MJ, Scholz CA (1993a) Estimating the age of formation of lakes: An example from Lake Tanganyika, East African Rift system. Geology 21:511. doi: 10.1130/0091-7613(1993)021<0511:etaofo>2.3.co;2

Cohen AS, Bills R, Cocquyt CZ, Caljon A (1993b) The impact of sediment pollution on biodiversity in Lake Tanganyika. Conserv Biol 7:667–677. doi: 10.1046/j.1523-1739.1993.07030667.x

Cohen AS, Kaufman L, Ogutu-Ohwayo R (1996) Anthropogenic threats, impacts and conservation strategies in the African Great Lakes — A review. In: Johnson T, Odada E (eds.) The Limnology, Climatology, and Paleoclimatology of the East African Lakes. Gordon & Breach Publ., Newark, NJ, 575-624

Cohen AS, Palacios-Fest MR, Msaky ES, Alin SR, McKee B, O'Reilly CM, Dettman DL, Nkotagu H, Lezzar KE (2005) Paleolimnological investigations of anthropogenic environmental change in Lake Tanganyika: IX. Summary of paleorecords of environmental change and catchment deforestation at Lake Tanganyika and impacts on the Lake Tanganyika ecosystem. J Paleolimnol 34:125–145. doi:10.1007/s10933-005-2422-4

Conaway CH, Swarzenski PW, Cohen AS (2012) Recent paleorecords document rising mercury contamination in Lake Tanganyika. Appl Geochem 27:352–359. doi: 10.1016/j.apgeochem.2011.11.005

Coulter GW (1991) Systematic composition of the flora and fauna. In: Coulter GW (ed.) Lake Tanganyika and its life. Oxford University Press, Oxford, pp 200–275

Coulter GW, Spiegel RH (1991) Hydrodynamics of Lake Tanganyika. In: Coulter GW (ed.) Lake Tanganyika and its life. Oxford University Press, Oxford, pp 49–75

Donohue I, Duck RW, Irvine K (2003) Land use, sediment loads and dispersal pathways from two catchments at the southern end of Lake Tanganyika, Africa: implications for lake management. Environ Geology 44:448–455. doi: 10.1007/s00254-003-0779-0

Donohue I, Irvine K (2004) Size-specific effects of increased sediment loads on gastropod communities in Lake Tanganyika, Africa. Hydrobiologia 522:337–342. doi: 10.1023/b:hydr.0000029969.44130.80

Donohue I, Molinos JG (2009) Impacts of increased sediment loads on the ecology of lakes. Biol Rev 84:517–531. doi: 10.1111/j.1469-185x.2009.00081.x

Drake N, Wooster M, Symeonakis E, Zhang X (1999) Soil erosion modeling in the Lake Tanganyika catchment (Technical Report Number 5). In: Pollution Control and Other Measures to Protect Biodiversity in Lake Tanganyika (RAF/92/G32), Kent, UK

Fire Effects Monitoring and Inventory Protocol (2004) The Normalized Burn Ratio (NBR) - brief outline of processing steps. FIREMON 4:1

García-Ruiz JM (2010) The effects of land uses on soil erosion in Spain: A review. Catena 81:1–11. doi: 10.1016/j.catena.2010.01.001

Geyer W, Hill P, Kineke G (2004) The transport, transformation and dispersal of sediment by buoyant coastal flows. Cont Shelf Res 24:927–949. doi: 10.1016/j.csr.2004.02.006

Hecky RE, Degens ET (1973) Late Pleistocene-Holocene chemical stratigraphy and paleolimnology of the Rift Valley lakes of Central Africa. W.H.O.I., Unpublished manuscript, Woods Hole, Massachusetts, WHOI-73-28:1–93

Hunink JE, Terink W, Contreras S, Droogers P (2015) Scoping Assessment of Erosion Levels for the Mahale region, Lake Tanganyika, Tanzania. FutureWater Report 148:1-47

Kabete J, Groves D, Mcnaughton N, Mruma A (2012) A new tectonic and temporal framework for the Tanzanian Shield: Implications for gold metallogeny and undiscovered endowment. Ore Geology Reviews 48:88–124. doi: 10.1016/j.oregeorev.2012.02.009

Kashaigilia JJ, Majaliwa AM (2013) Implications of land use and land cover changes on hydrological regimes of the Malagarasi River, Tanzania. J of Agric Science and Appl 02:45–50. doi: 10.14511/jasa.2013.020107

Lake Tanganyika Biodiversity Project (1998) Lake Tanganyika Biodiversity Project, http://www.ltbp.org/EINDEX.HTM (accessed February 2017)

Leloup E (1953) Exploration Hydrobiologique du Lac Tanganyika. Institut Royal des Sciences Naturelles de Belgique 3:1-273

Lezzar KE, Tiercelin J-J, Batist MD, Cohen AS, Bandora T, Van Rensbergen P, Le Turdu C, Mifundu W, Klerkx J (1996) New seismic stratigraphy and Late Tertiary history of the North Tanganyika Basin, East African Rift system, deduced from multichannel and high-resolution reflection seismic data and piston core evidence. Basin Research 8:1–28. doi: 10.1111/j.1365-2117.1996.tb00112.x

Manconi R, Pronzato R (2008) Global diversity of sponges (Porifera: Spongillina) in freshwater. Dev in Hydrobiol Freshwater Animal Divers Assess 27–33. doi: 10.1007/978-1-4020-8259-7_3

Maruyama A, Yuma M, Rusuwa B (2011) Impacts of sedimentation on the abundance and diversity of cichlid fishes in Lake Malawi. Soil Erosion: Causes, Processes and Effects 141–160

Mattheus CR, Rodriguez AB, Mckee BA (2009) Direct connectivity between upstream and downstream promotes rapid response of lower coastal-plain rivers to land use change. Geophys Res Letters 36:1-6. doi: 10.1029/2009gl039995

McGlue MM, Lezzar KE, Cohen AS, Russell JM, Tiercelin JJ, Felton, AA, Mbede E, Nkotagu HH (2008) Seismic records of late Pleistocene aridity in Lake Tanganyika, tropical East Africa. J of Paleolimnol 40:635–653. doi: 10.1007/s10933-007-9187-x

McGlue MM, Soreghan MJ, Michel E, Todd JA, Cohen AS, Mischler J, O'Connell CS, Castañeda OS, Hartwell RJ, Lezzar KE, Nkotagu HH (2010) Environmental controls on shell-rich facies in tropical lacustrine rifts: a view from Lake Tanganyika's littoral. Palaios 25:426–438. doi: 10.2110/palo.2009.p09-160r

McIntyre PB, Michel E, France K, Rivers A, Hakizimana P, Cohen AS (2005) Individual- and assemblage-level effects of anthropogenic sedimentation on snails in Lake Tanganyika. Conserv Biol 19:171–181. doi: 10.1111/j.1523-1739.2005.00456.x

Moore JES (1903) The Tanganyika problem: an account of the researches undertaken concerning the existence of marine animals in Central Africa. Hurst and Blackett, London, England

Montgomery DR, Brandon MT (2002) Topographic controls on erosion rates in tectonically active mountain ranges. Earth and Planet Sci Letters 201:481-489

Nkotagu H, Mbwambo K (1999), Hydrology of selected watersheds along the Lake Tanganyika shoreline (Technical Report Number 11). In: Pollution Control and Other Measures to Protect Biodiversity in Lake Tanganyika (RAF/92/G32), Kent, UK

Nsabimana S (1991) L'erosion des sols et la pollution du Lac Tanganyika au Burundi. In: Cohen AS (ed.) Report of the First International Conference on the Conservation and Biodiversity of Lake Tanganyika, Biodiversity Support Program, Washington, D.C.

Obi M, Salako F, Lal R (1989) Relative susceptibility of some southeastern Nigeria soils to erosion. Catena 16:215–225. doi: 10.1016/0341-8162(89)90009-x

Odigie KO, Cohen AS, Swarzenski PW, Flegal, AR (2014) Using lead isotopes and trace element records from two contrasting Lake Tanganyika sediment cores to assess watershed – Lake exchange. Appl Geochem 51:184–190. doi: 10.1016/j.apgeochem.2014.10.007

O'Reilly CM, Alin SR, Plisnier P-D, Cohen AS, McKee BA (2003) Climate change decreases aquatic ecosystem productivity of Lake Tanganyika, Africa. Nature 424:766–768. doi: 10.1038/nature01833

Orton GJ, Reading HG (1993) Variability of deltaic processes in terms of sediment supply, with particular emphasis on grain size. Sedimentology 40:475–512. doi: 10.1111/j.1365-3091.1993.tb01347.x

Palacios-Fest MR, Cohen AS, Lezzar K, Nahimana L, Tanner BM (2005) Paleolimnological investigations of anthropogenic environmental change in Lake Tanganyika: III. Physical stratigraphy and charcoal analysis. J of Paleolimnol 34:31–49. doi: 10.1007/s10933-005-2396-2

Patterson G (2000) Summary of findings for the Strategic Action Programme (SAP). In: Pollution Control and Other Measures to Protect Biodiversity in Lake Tanganyika (RAF/92/G32), Kent, UK

Plisnier P-D, Chitamwebwa D, Mwape L, Tshibangu K, Langenberg V, Coenen E (1999) Limnological annual cycle inferred from physical-chemical fluctuations at three stations of Lake Tanganyika. From Limnology to Fisheries: Lake Tanganyika and Other Large Lakes 45–58. doi: 10.1007/978-94-017-1622-2_4

Rossiter A (1995) The cichlid fish assemblages of Lake Tanganyika: ecology, behaviour and evolution of its species flocks. Adv Ecol Res 26:187–252

Rosendahl BR, Reynolds DJ, Lorber PM, Burgess CF, McGill J, Scott D, Lambiase JJ, Derksen SJ (1986) Structural expressions of rifting: lessons from Lake Tanganyika, Africa. Geological Society, London, Special Publications 25:29–43. doi: 10.1144/gsl.sp.1986.025.01.04

Sato T (1994) Active accumulation of spawning substrate: a determinant of extreme polygyny in a shell-brooding cichlid fish. Anim Behav 48:669–678. doi:10.1006/anbe.1994.1286

Sengupta ME, Kristensen TK, Madsen H, Jørgensen A (2009) Molecular phylogenetic investigations of the Viviparidae (Gastropoda: Caenogastropoda) in the lakes of the Rift Valley area of Africa. Mol Phylogenet and Evol 52:797–805. doi: 10.1016/j.ympev.2009.05.007

Soreghan MJ, Cohen AS (1996) Textural and compositional variability across littoral segments of Lake Tanganyika: the effect of asymmetric basin structure on sedimentation in large rift lakes. Am Assoc Pet Geol Bull 80:382–409

Soreghan MJ (2016) Conservation implications of the provenance of modern sediment on a shell-rich platform of Lake Tanganyika (Kigoma, TZ). Environ Earth Sci. doi: 10.1007/s12665-016-5662-x

USDA Foreign Agricultural Service, NASA, SGT, UMD (2017) Lake Tanganyika (0315) Height Variations from TOPEX/POSEIDON/Jason-1 and Jason-2/OSTM Altimetry. https://www.pecad.fas.usda.gov/cropexplorer/global_reservoir/gr_regional_chart.aspx?regionid=safrica&reservoir_name=Tanganyika

U.S. Geological Survey (2016) Landsat 8 Data Users Handbook. EROS. Sioux Falls, SD

Van Damme D, Pickford M (1999) The late Cenozoic Viviparidae (Mollusca, Gastropoda) of the Albertine Rift Valley. Hydrobiologia 390:171–217

Verburg P, Antenucci JP, Hecky RE (2011) Differential cooling drives large-scale convective circulation in Lake Tanganyika. Limnol and Oceanogr 56:910–926. doi: 10.4319/lo.2011.56.3.0910

Verburg P, Huttula T, Kakogozo B, Kihakwi A, Kotilainen P, Makasa L, Peltonen A (1997) Hydrodynamics of Lake Tanganyika and meteorological results (GCP/RAF/271/FIN-TD/59). In: Research for the Tanganyika Management of Fisheries on Lake Tanganyika, FAO/FINNIDA, Bujumbura, Burundi

Walling D, Fang D (2003) Recent trends in the suspended sediment loads of the world's rivers. Glob and Planet Change 39:111–126. doi: 10.1016/s0921-8181(03)00020-1

Walling DE, Owens PN, Foster IDL, Lees JA (2003) Changes in the fine sediment dynamics of the Ouse and Tweed basins in the UK over the last 100-150 years. Hydrol Process 17:3245–3269. doi: 10.1002/hyp.1385

West K, Cohen A, Baron M (1991) Morphology and behavior of crabs and gastropods from Lake Tanganyika, Africa: Implications for lacustrine predator-prey coevolution. Evolution 45:589. doi: 10.2307/2409913

Appendix A: LPSA Operation Methodology

The Malvern Mastersizer 3000 laser particle size analyzer was used with the small volume sample dispersion unit for the mud fraction grain size analysis. Prior to analysis, 2-3 drops of sodium hexametaphosphate (NaMP) were added to the 10 mL vials containing the mud samples (and DI water), and the vials were then sonicated for 1-2 minutes. After turning on the Mastersizer 3000 and allowing the instrument to warm up for 30 minutes, the small volume dispersion unit was filled with distilled water and rinsed several times. Using the Mastersizer 3000 software, background values were checked to ensure that the unit was clean prior to adding any sample to the dispersion unit. Once samples were sonicated and the proper steps were taken to ensure that the instrument was clean and running correctly, samples were added to the dispersion unit (running at ~2500 RPM) one drop at a time using a clean pipette. Sample was continuously added to the dispersion unit until obscuration requirements were met (0-24%). Once the obscuration was in range, the measurement was taken using the software and the results were saved. After each sample was analyzed, the sample dispersion unit was rinsed three separate times with distilled water, and then refilled prior to measuring the next sample. Raw data and histograms were exported into an excel spreadsheet after the analyses were complete.

Appendix B: Land Cover Methodology from Daniel Kelly (TNC)

We collected Landsat satellite imagery data from the United States Geological Survey's Earth Explorer website (http://earthexplorer.usgs.gov/). Both Landsat 7 ETM+ (L7) and Landsat 8 OLI (L8) multispectral data were selected for the change analysis and have a spatial resolution of 30 meters. In selecting images we tried to reduce the impact of cloud cover as much as possible and therefore the acquisition dates for the images reflect that constraint. The Landsat scenes used in the analysis were path, row combinations: 172,064; 172,065; 171,064 and 171,065. For path 172 the dates used in the analysis were October 1, 2001 (L7) and October 13, 2014 (L8). For path 171 we used September 24, 2001 (L7) and October 13, 2014 (L8).

ERDAS Imagine 2015 software was used to perform the analysis. We used a supervised classification approach with a maximum likelihood decision rule. In order to run the supervised classification we developed a set of spectral signatures for each land cover class based on prior field visits and ground points collected using GPS. These signatures were then entered into the software to perform the classification. This was an iterative approach where the results of a classification we compared to high resolution imagery using Google Earth (GE). Areas that did not classify correctly had signatures added or modified until a satisfactory result was achieved. We also segmented the image into zones of similar land cover to reduce the chance of mixed pixels between different land cover types.

To improve the classification accuracy we made alterations to it using visual interpretation methods in GE. An example of this is the settlement class. Due to the sparse nature of many rural settlements, the inclusion of vegetation between structures

and the spatial resolution of the satellite data we had poor classification accuracy of the settlement class. These changes were made where it was clear that the automated classification methods could not produce satisfactory results.

The final classification was then run through a 3x3 majority filter to smooth the results and remove individual isolated pixels.

Appendix C: Summary of Sediment Plume Area Calculations

		Katumbi		Lagosa		Rukoma	
Image Date	Sensor	Plume Size (km^2)	Plume Direction and Appearance	Plume Size (km^2)	Plume Direction and Appearance	Plume Size (km^2)	Plume Direction and Appearance
5/11/2016	Landsat 8	0	plume not visible	1.845	plume deflected to the east with some turbid water to the southwest	2.9295	plume equally deflected east and west
3/6/2015	Landsat 8	0	plume not visible	1.4796	plume equally deflected east and west	2.6181	plume deflected to east
3/3/2014	Landsat 8	0.5121	plume deflected more to west and some to east	2.5821	plume equally deflected east and west	2.8674	deflected mostly to west some to east
1/30/2014	Landsat 8	n/a	delta obscured by clouds	3.1131	plume equally deflected east and west	n/a	delta obscured by clouds
5/19/2013	Landsat 8	0	plume not visible	2.826	plume equally deflected east and west	2.934	deflected mostly to west some to east
5/13/2002	Landsat 7	0	plume not visible	1.2024	plume equally deflected east and west	1.5228	plume equally deflected east and west
2/22/2002	Landsat 7	0	plume not visible	1.215	plume deflected more to east but also some to west	1.0593	deflected to west
2/3/2001	Landsat 7	0.4347	plume equally deflected east and west	1.5066	plume equally deflected east and west	1.701	deflected mostly to west some to east
4/21/2000	Landsat 7	0	plume not visible	0.9279	plume equally deflected east and west	1.8036	deflected mostly to west some to east
12/31/1999	Landsat 7	0	visible but unable to be classified (not dense enough)	2.4795	deflected mostly to east some to west	4.3056	plume equally deflected east and west
3/1/1996	Landsat 5	0	plume not visible	1.9116	plume equally deflected east and west	2.8242	deflected mostly to west some to east
4/29/1994	Landsat 5	0	plume not visible	1.2834	plume equally deflected east and west	2.1177	deflected mostly to west some to east
10/30/1991	Landsat 5	0	plume not visible	2.5722	deflected to east (most dense plume seen for all images)	4.3092	deflected mostly to east (most dense plume seen for all images)

Appendix D: Summary Metadata for Landsat Imagery

Image Date	Scene ID	Sensor	Path	Row
8/31/2016	LC81720642016244LGN00	Landsat 8 OLI/TIRS	172	64
7/30/2016	LC81720642016212LGN00	Landsat 8 OLI/TIRS	172	64
5/27/2016	LC81720642016148LGN00	Landsat 8 OLI/TIRS	172	64
5/11/2016	LC81720642016132LGN00	Landsat 8 OLI/TIRS	172	64
8/13/2015	LC81720642015225LGN00	Landsat 8 OLI/TIRS	172	64
6/10/2015	LC81720642015161LGN00	Landsat 8 OLI/TIRS	172	64
4/7/2015	LC81720642015097LGN00	Landsat 8 OLI/TIRS	172	64
3/6/2015	LC81720642015065LGN00	Landsat 8 OLI/TIRS	172	64
8/10/2014	LC81720642014222LGN00	Landsat 8 OLI/TIRS	172	64
5/22/2014	LC81720642014142LGN00	Landsat 8 OLI/TIRS	172	64
3/3/2014	LC81720642014062LGN00	Landsat 8 OLI/TIRS	172	64
1/30/2014	LC81720642014030LGN00	Landsat 8 OLI/TIRS	172	64
8/23/2013	LC81720642013235LGN00	Landsat 8 OLI/TIRS	172	64
7/6/2013	LC81720642013187LGN00	Landsat 8 OLI/TIRS	172	64
6/4/2013	LC81720642013155LGN00	Landsat 8 OLI/TIRS	172	64
5/19/2013	LC81720642013139LGN01	Landsat 8 OLI/TIRS	172	64
4/22/2012	LE71720642012113ASN00	Landsat 7 ETM+	172	64
3/21/2012	LE71720642012081ASN00	Landsat 7 ETM+	172	64
2/2/2012	LE71720642012033ASN00	Landsat 7 ETM+	172	64
7/25/2011	LE71720642011206ASN00	Landsat 7 ETM+	172	64
5/30/2011	LT51720642011150JSA00	Landsat 5 TM	172	64
4/4/2011	LE71720642011094ASN00	Landsat 7 ETM+	172	64
8/7/2010	LE71720642010219ASN00	Landsat 7 ETM+	172	64
7/6/2010	LE71720642010187ASN00	Landsat 7 ETM+	172	64

5/27/2010	LT51720642010147JSA01	Landsat 5 TM	172	64
7/3/2009	LE71720642009184ASN00	Landsat 7 ETM+	172	64
5/24/2009	LT51720642009144JSA01	Landsat 5 TM	172	64
5/16/2009	LE71720642009136ASN00	Landsat 7 ETM+	172	64
2/25/2009	LE71720642009056ASN00	Landsat 7 ETM+	172	64
12/7/2008	LE71720642008342ASN00	Landsat 7 ETM+	172	64
8/9/2008	LT51720642008222JSA00	Landsat 5 TM	172	64
7/16/2008	LE71720642008198ASN00	Landsat 7 ETM+	172	64
5/5/2008	LT51720642008126JSA00	Landsat 5 TM	172	64
12/21/2007	LE71720642007355ASN00	Landsat 7 ETM+	172	64
8/31/2007	LE71720642007243ASN00	Landsat 7 ETM+	172	64
8/7/2007	LT51720642007219JSA00	Landsat 5 TM	172	64
3/24/2007	LE71720642007083ASN03	Landsat 7 ETM+	172	64
2/20/2007	LE71720642007051ASN00	Landsat 7 ETM+	172	64
8/12/2006	LE71720642006224ASN00	Landsat 7 ETM+	172	64
5/24/2006	LE71720642006144ASN00	Landsat 7 ETM+	172	64
4/22/2006	LE71720642006112ASN00	Landsat 7 ETM+	172	64
10/12/2005	LE71720642005285ASN00	Landsat 7 ETM+	172	64
9/2/2005	LT51720642005245JSA00	Landsat 5 TM	172	64
8/25/2005	LE71720642005237ASN00	Landsat 7 ETM+	172	64
7/16/2005	LT51720642005197JSA00	Landsat 5 TM	172	64
6/14/2005	LT51720642005165JSA00	Landsat 5 TM	172	64
5/21/2005	LE71720642005141ASN01	Landsat 7 ETM+	172	64
7/5/2004	LE71720642004187ASN01	Landsat 7 ETM+	172	64
6/3/2004	LE71720642004155ASN01	Landsat 7 ETM+	172	64
4/16/2004	LE71720642004107ASN01	Landsat 7 ETM+	172	64
7/19/2003	LE71720642003200ASN01	Landsat 7 ETM+	172	64

3/13/2003	LE71720642003072JSA00	Landsat 7 ETM+	172	64
2/25/2003	LE71720642003056SGS00	Landsat 7 ETM+	172	64
8/17/2002	LE71720642002229EDC00	Landsat 7 ETM+	172	64
6/30/2002	LE71720642002181JSA00	Landsat 7 ETM+	172	64
5/13/2002	LE71720642002133SGS00	Landsat 7 ETM+	172	64
2/22/2002	LE71720642002053SGS00	Landsat 7 ETM+	172	64
3/7/2001	LE71720642001066SGS00	Landsat 7 ETM+	172	64
2/3/2001	LE71720642001034SGS00	Landsat 7 ETM+	172	64
8/27/2000	LE71720642000240SGS00	Landsat 7 ETM+	172	64
4/21/2000	LE71720642000112SGS00	Landsat 7 ETM+	172	64
12/31/1999	LE71720641999365EDC00	Landsat 7 ETM+	172	64
7/23/1996	LT51720641996205JSA00	Landsat 5 TM	172	64
6/5/1996	LT51720641996157JSA00	Landsat 5 TM	172	64
3/1/1996	LT51720641996061JSA01	Landsat 5 TM	172	64
9/7/1995	LT51720641995250JSA00	Landsat 5 TM	172	64
6/19/1995	LT51720641995170JSA00	Landsat 5 TM	172	64
8/3/1994	LT51720641994215JSA00	Landsat 5 TM	172	64
4/29/1994	LT51720641994119JSA00	Landsat 5 TM	172	64
7/15/1993	LT51720641993196JSA00	Landsat 5 TM	172	64
8/29/1992	LT51720641992242JSA00	Landsat 5 TM	172	64
10/30/1991	LT51720641991303JSA00	Landsat 5 TM	172	64
8/11/1991	LT51720641991223JSA00	Landsat 5 TM	172	64
7/23/1990	LT51720641990204JSA00	Landsat 5 TM	172	64
9/22/1989	LT51720641989265JSA01	Landsat 5 TM	172	64
2/5/1987	LT51720641987036XXX01	Landsat 5 TM	172	64
7/28/1986	LT51720641986209XXX03	Landsat 5 TM	172	64
10/10/1984	LT51720641984284XXX02	Landsat 5 TM	172	64

Appendix E: Grain-Size Data Summary

Sample Number	Transect	Depth (m)	mass of dry sediment (g)			total mass (g)	weight % of bulk sample		
			gravel	sand	mud		gravel	sand	mud
MT2016-T12-03	MT12	3	0.05	30.62	1.72	32.39	0.15	94.54	5.31
MT2016-T12-06	MT12	6	0.00	39.71	5.07	44.78	0.00	88.68	11.32
MT2016-T12-09	MT12	9	0.00	20.25	8.29	28.54	0.00	70.95	29.05
MT2016-T12-12	MT12	12	0.00	22.57	8.64	31.21	0.00	72.32	27.68
MT2016-T12-15	MT12	15	0.02	24.85	9.97	34.84	0.06	71.33	28.62
MT2016-T12-20	MT12	20	35.43	44.18	2.90	82.51	42.94	53.55	3.51
MT2016-T12-30	MT12	30	26.14	18.66	5.86	50.66	51.60	36.83	11.57
MT2016-T12-40	MT12	40	1.40	3.86	4.48	9.74	14.37	39.63	46.00
MT2016-T12-50	MT12	50	1.83	14.97	17.88	34.68	5.28	43.17	51.56
MT2016-T12-60	MT12	60	11.82	5.96	17.06	34.84	33.93	17.11	48.97
MT2016-T09-03	MT9	3	0.24	37.04	0.20	37.48	0.64	98.83	0.53
MT2016-T09-09	MT9	9	1.34	45.19	0.17	46.70	2.87	96.77	0.36
MT2016-T09-12	MT9	12	0.07	34.17	0.38	34.62	0.20	98.70	1.10
MT2016-T09-15	MT9	15	4.29	32.86	0.37	37.52	11.43	87.58	0.99
MT2016-T09-30	MT9	30	12.74	39.00	1.17	52.91	24.08	73.71	2.21
MT2016-T09-40	MT9	40	9.79	46.72	0.49	57.00	17.18	81.96	0.86
MT2016-T08-03	MT8	3	0.00	44.29	0.21	44.50	0.00	99.53	0.47
MT2016-T08-06	MT8	6	6.84	47.36	0.26	54.46	12.56	86.96	0.48
MT2016-T08-09	MT8	9	5.26	42.45	0.31	48.02	10.95	88.40	0.65
MT2016-T08-12	MT8	12	0.17	32.17	0.38	32.72	0.52	98.32	1.16
MT2016-T08-15	MT8	15	0.03	30.96	1.08	32.07	0.09	96.54	3.37
MT2016-T08-20	MT8	20	5.21	24.33	2.71	32.25	16.16	75.44	8.40
MT2016-T08-30	MT8	30	0.69	33.85	5.28	39.82	1.73	85.01	13.26
MT2016-T08-40-2	MT8	40	30.94	0.40	0.42	31.76	97.42	1.26	1.32

MT2016-T13-03	MT13	3	0.04	34.37	0.53	34.94	0.11	98.37	1.52
MT2016-T13-06	MT13	6	3.69	42.37	1.00	47.06	7.84	90.03	2.12
MT2016-T13-09	MT13	9	5.08	45.75	0.79	51.62	9.84	88.63	1.53
MT2016-T13-12	MT13	12	0.06	43.78	2.50	46.34	0.13	94.48	5.39
MT2016-T13-15	MT13	15	6.93	40.89	4.18	52	13.33	78.63	8.04
MT2016-T13-20	MT13	20	37.95	31.08	4.95	73.98	51.30	42.01	6.69
MT2016-T13-30	MT13	30	12.00	18.03	1.77	31.8	37.74	56.70	5.57
MT2016-T13-40	MT13	40	0.98	39.05	4.75	44.78	2.19	87.20	10.61
MT2016-T10-03	MT10	3	0.06	39.41	0.96	40.43	0.15	97.48	2.37
MT2016-T10-06	MT10	6	1.36	14.88	11.79	28.03	4.85	53.09	42.06
MT2016-T10-09	MT10	9	0.20	30.81	11.31	42.32	0.47	72.80	26.72
MT2016-T10-12	MT10	12	1.65	26.64	12.51	40.8	4.04	65.29	30.66
MT2016-T10-15	MT10	15	4.28	35.14	12.18	51.6	8.29	68.10	23.60
MT2016-T10-20	MT10	20	0.14	20.82	12.45	33.41	0.42	62.32	37.26
MT2016-T10-30	MT10	30	0.14	46.70	14.79	61.63	0.23	75.77	24.00
MT2016-T10-40	MT10	40	0.95	33.75	6.74	41.44	2.29	81.44	16.26
MT2016-T14-03	MT14	3	0.64	59.47	0.29	60.4	1.06	98.46	0.48
MT2016-T14-06	MT14	6	8.84	39.79	1.49	50.12	17.64	79.39	2.97
MT2016-T14-09	MT14	9	0.08	28.53	4.42	33.03	0.24	86.38	13.38
MT2016-T14-12	MT14	12	0.13	32.10	7.98	40.21	0.32	79.83	19.85
MT2016-T14-15	MT14	15	0.14	24.06	9.77	33.97	0.41	70.83	28.76
MT2016-T14-20	MT14	20	67.05	3.84	1.93	72.82	92.08	5.27	2.65
MT2016-T14-30	MT14	30	31.98	19.81	0.35	52.14	61.33	37.99	0.67
MT2016-T14-40	MT14	40	20.36	29.95	3.56	53.87	37.79	55.60	6.61
MT2016-T15-03	MT15	3	0.00	42.18	2.80	44.98	0.00	93.78	6.22
MT2016-T15-06	MT15	6	0.24	9.89	19.98	30.11	0.80	32.85	66.36
MT2016-T15-09	MT15	9	0.41	13.23	21. 85	35.49	1.16	37.28	61.57
MT2016-T15-12	MT15	12	0.08	13.85	19.68	33.61	0.24	41.21	58.55

MT2016-T15-15	MT15	15	0.01	13.58	19.06	32.65	0.03	41.59	58.38
MT2016-T15-20	MT15	20	0.01	9.44	24.72	34.17	0.03	27.63	72.34
MT2016-T15-30	MT15	30	44.19	40.21	7.60	92	48.03	43.71	8.26
MT2016-T15-40	MT15	40	14.41	15.02	0.74	30.17	47.76	49.78	2.45
Katato R-1	onshore	onshore	0.07	12.21	46.18	58.46	0.12	20.89	78.99
Katato R-2	onshore	onshore	0.05	4.39	11.80	16.24	0.31	27.01	72.67
Lagosa River -1 Bar	onshore	onshore	18.86	200.16	2.02	221.04	8.53	90.56	0.91
Lagosa River-2 Mud-Pt. Bar	onshore	onshore	3.08	43.17	29.43	75.68	4.07	57.05	38.89
Lagosa River-3 Overbank Levee	onshore	onshore	8.31	70.16	25.47	103.94	7.99	67.50	24.50
Lagosa River-4	onshore	onshore	0.12	22.77	25.72	48.60	0.24	46.84	52.92
MT2015-Live Neoth.	Katumbi		2.83	81.33	10.43	94.59	2.99	85.98	11.03
LT2015-MT3-3D	MT3	3	0.33	74.85	0.83	76.01	0.44	98.47	1.09
MT2015-T3-06	MT3	6	14.47	15.44	9.04	38.95	37.15	39.64	23.21
LT2015-MT3-9D	MT3	9	15.64	8.84	3.74	28.22	55.43	31.32	13.25
LT2015-MT3-12D	MT3	12	10.04	14.13	7.61	31.78	31.60	44.45	23.95
LT2015-MT3-15D	MT3	15	15.78	13.58	4.55	33.91	46.54	40.05	13.42
LT2015-MT3-20D	MT3	20	7.48	2.04	9.04	18.55	40.30	10.97	48.72
MT2015-T3-30PB	MT3	30	16.82	21.11	8.99	46.92	35.85	45.00	19.16
LT2015-MT3-40PA	MT3	40	8.87	43.98	5.39	58.24	15.23	75.52	9.25
LT2015-MT1-3D	MT1	3	0.03	51.89	0.34	52.26	0.06	99.29	0.65
LT2015-MT1-6D	MT1	6	0.67	86.61	0.22	87.50	0.76	98.98	0.25
LT2015-MT1-9D	MT1	9	17.02	3.11	0.33	20.46	83.19	15.20	1.61
LT2015-MT1-12D	MT1	12	27.73	6.24	1.67	35.64	77.81	17.50	4.69
LT2015-MT1-15D	MT1	15	37.45	10.81	0.74	48.99	76.43	22.06	1.51
LT2015-MT1-20D	MT1	20	53.24	0.88	0.19	54.31	98.02	1.63	0.35
MT2015-T1-30PB	MT1	30	55.38	20.04	0.70	76.12	72.75	26.33	0.92

MT2015-T1-40PB	MT1	40	3.30	22.28	0.79	26.36	12.50	84.50	3.00
MT2015-T2-03	MT2	3	0.03	35.30	7.42	42.75	0.07	82.57	17.36
MT2015-T2-06	MT2	6	0.02	26.96	8.35	35.33	0.06	76.31	23.63
MT2015-T2-09	MT2	9	1.93	45.45	50.06	97.44	1.98	46.64	51.38
MT2015-T2-12	MT2	12	0.04	4.78	14.16	18.98	0.21	25.18	74.60
MT2015-T2-15	MT2	15	0.21	19.28	63.24	82.73	0.25	23.30	76.44
LT2015-MT2-20D	MT2	20	0.32	27.73	41.55	69.60	0.46	39.85	59.70
MT2015-T2-30	MT2	30	38.56	28.20	6.87	73.63	52.37	38.30	9.33
MT2015-T2-40	MT2	40	22.21	52.88	3.56	78.65	28.24	67.23	4.53
MT2015-T2-50P	MT2	50	2.68	45.27	2.04	49.99	5.36	90.56	4.08
MT2015-T2-60P	MT2	60	1.15	25.72	0.74	27.61	4.18	93.14	2.68
MT2015-T5-03	MT5	3	0.01	16.42	17.07	33.5	0.03	49.01	50.96
LT2015-MT5-6D	MT5	6	5.44	14.48	4.08	24.00	22.67	60.33	17.00
LT2015-MT5-9D	MT5	9	0.00	6.16	7.09	13.25	0.00	46.51	53.49
LT2015-MT5-12D	MT5	12	0.82	11.06	8.94	20.82	3.94	53.13	42.93
LT2015-MT5-15D	MT5	15	8.04	26.49	2.72	37.26	21.59	71.11	7.30
LT2015-MT5-20D	MT5	20	28.36	6.96	2.20	37.52	75.58	18.55	5.86
MT2015-T5-30P-A	MT5	30	48.07	1.51	0.12	49.7	96.72	3.04	0.24
MT2015-T5-40P-B	MT5	40	24.54	1.04	0.11	25.69	95.52	4.05	0.43
MT2015-T6-06	MT6	6	31.08	21.94	7.98	61	50.95	35.97	13.08
LT2015-MT6-9D	MT6	9	20.56	19.05	4.22	43.83	46.91	43.46	9.63
MT2015-T6-12	MT6	12	48.52	3.67	2.11	54.3	89.36	6.76	3.89
LT2015-MT6-15D	MT6	15	48.99	9.53	0.13	58.65	83.53	16.25	0.22
LT2015-MT6-20D	MT6	20	39.17	24.58	0.90	64.65	60.58	38.02	1.39
MT2015-T6-30P	MT6	30	16.38	13.95	1.39	31.72	51.64	43.98	4.38
MT2015-T6-40P	MT6	40	0.10	39.90	0.00	40.00	0.25	99.75	0.00
MT2015-T6-50P	MT6	50	7.78	35.17	0.80	43.75	17.78	80.39	1.83
MT2015-T6-60P	MT6	60	18.35	29.31	0.63	48.29	38.00	60.70	1.30

MT2015-T4-03	MT4	3	0.48	118.08	0.74	119.3	0.40	98.98	0.62
MT2015-T4-06	MT4	6	20.00	97.57	0.23	117.8	16.98	82.83	0.20
MT2015-T4-09	MT4	9	31.97	141.60	0.66	174.23	18.35	81.27	0.38
LT2015-MT4-12D	MT4	12	31.47	2.85	0.58	34.90	90.16	8.17	1.66
LT2015-MT4-15D	MT4	15	19.89	0.96	0.16	21.01	94.69	4.55	0.76
LT2015-MT4-20D	MT4	20	20.43	0.96	0.05	21.45	95.28	4.49	0.23
MT2015-T4-30P-B	MT4	30	12.32	45.71	0.96	58.99	20.88	77.49	1.63
MT2015-T4-40PB	MT4	40	41.22	23.42	1.01	65.65	62.79	35.67	1.54
MT2015-T4-50P	MT4	50	10.92	57.12	2.45	70.49	15.49	81.03	3.48
MT2015-T4-60P	MT4	60	2.73	82.25	3.89	88.87	3.07	92.55	4.38
MT2015-T7-03	MT7	3	0.61	111.52	1.89	114.02	0.53	97.81	1.66
MT2015-T7-06	MT7	6	18.00	77.24	0.79	96.03	18.74	80.43	0.82
LT2015-MT7-9D	MT7	9	31.61	7.71	1.52	40.84	77.41	18.87	3.72
LT2015-MT7-12D	MT7	12	16.55	15.50	1.86	33.91	48.81	45.71	5.48
LT2015-MT7-15D	MT7	15	41.16	29.29	1.77	72.21	56.99	40.56	2.45
MT2015-T7-20	MT7	20	35.92	13.37	2.83	52.12	68.92	25.65	5.43
MT2015-T7-30P	MT7	30	71.71	3.64	0.49	75.84	94.55	4.80	0.65
MT2015-T7-40P	MT7	40	56.09	1.15	1.56	58.8	95.39	1.96	2.65
MT2016-T11-03	MT11	3	0.00	34.28	0.16	34.44	0.00	99.54	0.46
MT2016-T11-06	MT11	6	2.31	43.62	0.07	46.00	5.02	94.83	0.15
MT2016-T11-09	MT11	9	2.00	55.63	0.23	57.86	3.46	96.15	0.40
MT2016-T11-12	MT11	12	0.40	52.14	0.48	53.02	0.75	98.34	0.91
MT2016-T11-15	MT11	15	9.81	26.62	0.49	36.92	26.57	72.10	1.33
MT2016-T11-20	MT11	20	0.31	35.49	2.23	38.03	0.82	93.32	5.86
MT2016-T11-30	MT11	30	1.72	41.05	1.96	44.73	3.85	91.77	4.38
MT2016-T11-40	MT11	40	6.70	40.73	1.45	48.88	13.71	83.33	2.97

MT2016-T11-50	MT11	50	0.49	12.96	0.03	13.48	3.64	96.14	0.22
MT2016-T11-60	MT11	60	8.38	49.43	1.62	59.43	14.10	83.17	2.73
MT2015-TLA-03	TLA	3	0.13	39.23	22.98	62.34	0.21	62.93	36.86
MT2015-TLA-06	TLA	6	0.05	7.70	13.23	20.98	0.24	36.70	63.06
MT2015-TLA-09	TLA	9	0.03	25.08	36.71	61.82	0.05	40.57	59.38
MT2015-TLA-12	TLA	12	0.12	53.50	45.80	99.42	0.12	53.81	46.07
MT2015-TLA-15	TLA	15	0.03	46.35	23.76	70.14	0.04	66.08	33.88
MT2015-TLA-20	TLA	20	0.37	52.13	33.23	85.73	0.43	60.81	38.76
MT2015-LAR-1	onshore	onshore	0.01	9.64	23.33	32.98	0.03	29.23	70.74
MT2015-LAR-2	onshore	onshore	0.07	20.07	12.31	32.45	0.22	61.85	37.94
MT2015-LAR-3	onshore	onshore	13.53	31.18	17.16	61.87	21.87	50.40	27.74
MT2015-LAR-4	onshore	onshore	1.85	33.50	8.48	43.83	4.22	76.43	19.35
MT2015-LAR-5	onshore	onshore	6.12	72.67	0.35	79.14	7.73	91.82	0.44
MT2016-LAR-1	onshore	onshore	4.35	13.51	7.50	25.36	17.15	53.27	29.57
MT2016-LAR-2	onshore	onshore	0.08	9.31	7.91	17.3	0.46	53.82	45.72
MT2016-LAR-3	onshore	onshore	0.01	3.77	9.74	13.52	0.07	27.88	72.04
MT2016-LAR-4	onshore	onshore	0.01	13.59	2.04	15.64	0.06	86.89	13.04
MT2016-LAR-5	onshore	onshore	0.23	5.39	8.64	14.26	1.61	37.80	60.59
2016-KbR-RM	onshore	onshore	0.53	50.29	0.07	50.89	1.04	98.82	0.14
2016-KbR-RM-2	onshore	onshore	13.71	37.18	0.14	51.03	26.87	72.86	0.27
2016-Beach-1	onshore	onshore	2.78	31.90	0.05	34.73	8.00	91.85	0.14
2016-Ngk-1	onshore	onshore	0.02	15.41	4.91	20.34	0.10	75.76	24.14
2016-Ngk-2	onshore	onshore	19.71	28.32	1.17	49.2	40.06	57.56	2.38
2016-Ngk-3	onshore	onshore	7.43	33.37	1.61	42.41	17.52	78.68	3.80
2016-KbR-1	onshore	onshore	13.91	16.78	0.83	31.52	44.13	53.24	2.63
2016-KbR-2	onshore	onshore	0.96	15.71	2.33	19	5.05	82.68	12.26
2016-KbR-3	onshore	onshore	0.10	12.39	6.01	18.5	0.54	66.97	32.49
2016-KbR-4	onshore	onshore	0.10	17.56	1.14	18.8	0.53	93.40	6.06
2016-KbR-5	onshore	onshore	38.60	7.22	0.06	45.88	84.13	15.74	0.13

2016-KbR-6	onshore	onshore	0.00	13.15	5.02	18.17	0.00	72.37	27.63
2016-KbR-7	onshore	onshore	0.01	8.19	2.76	10.96	0.09	74.73	25.18
2016-KbR-8	onshore	onshore	0.00	20.74	0.28	21.02	0.00	98.67	1.33
2016-KbR-9	onshore	onshore	0.45	21.20	0.10	21.75	2.07	97.47	0.46
2016-KbR-10	onshore	onshore	0.00	7.63	3.03	10.66	0.00	71.58	28.42
2016-KbR-mud-1	onshore	onshore	0.00	1.17	3.47	4.64	0.00	25.22	74.78
2016-KbR-mud-2	onshore	onshore	0.03	1.66	4.11	5.8	0.52	28.62	70.86
2016-KbR-mud-3	onshore	onshore	0.04	1.83	3.99	5.86	0.68	31.23	68.09
2016-KbR-mud-4	onshore	onshore	0.00	1.33	3.86	5.19	0.00	25.63	74.37
2016-KbR-mud-5	onshore	onshore	0.00	1.91	4.48	6.39	0.00	29.89	70.11
2016-KbR-mud-6	onshore	onshore	0.16	1.48	7.62	9.26	1.73	15.98	82.29

Appendix F: Loss on Ignition (LOI) Data Summary

Sample #	Depth	Transect	*after 550 burn*		*after 900 burn*		Total Net Wt Lost	Total % Lost
			Net wt lost (g)	% Lost	Net wt lost (g)	% Lost		
LT2015-MT1-3D	3	T1	0.043	1.4	0.165	11.7	0.208	6.8
LT2015-MT1-6D	6	T1	0.044	1.7	0.152	9.1	0.196	7.5
LT2015-MT1-9D	9	T1	0.112	5.4	0.472	8.7	0.584	28.2
LT2015-MT1-12D	12	T1	0.121	5.0	0.612	12.3	0.733	30.3
LT2015-MT1-15D	15	T1	0.081	3.8	0.638	16.8	0.719	33.7
LT2015-MT1-20D	20	T1	0.088	3.7	0.919	25.0	1.007	42.0
MT2015-T1-30PB	30	T1	0.087	3.1	0.67	21.7	0.757	26.9
MT2015-T1-40PB	40	T1	0.084	3.5	0.212	6.1	0.296	12.3
MT2016-T10-03	3	T10	0.017	0.5	0.021	0.7	0.038	1.2
MT2016-T10-06	6	T10	0.329	13.7	0.015	0.7	0.344	14.3
MT2016-T10-09	9	T10	0.164	3.7	0.036	0.9	0.2	4.5
MT2016-T10-12	12	T10	0.21	8.5	0.021	0.9	0.231	9.4
MT2016-T10-15	15	T10	0.155	5.6	0.025	1.0	0.18	6.5
MT2016-T10-20	20	T10	0.144	3.9	0.038	1.1	0.182	4.9
MT2016-T10-30	30	T10	0.099	2.3	0.054	1.3	0.153	3.5
MT2016-T10-40	40	T10	0.059	1.5	0.145	3.7	0.204	5.2
MT2016-T11-03	3	T11	0.037	0.8	0.041	0.8	0.078	1.6
MT2016-T11-06	6	T11	0.069	1.2	0.275	4.9	0.344	6.1
MT2016-T11-09	9	T11	0.041	0.9	0.053	1.2	0.094	2.1
MT2016-T11-12	12	T11	0.055	1.0	0.057	1.1	0.112	2.1
MT2016-T11-15	15	T11	0.048	1.4	0.269	7.8	0.317	9.1
MT2016-T11-20	20	T11	0.057	1.6	0.043	1.2	0.1	2.8
MT2016-T11-30	30	T11	0.074	1.4	0.406	7.8	0.48	9.1
MT2016-T11-40	40	T11	0.052	1.3	0.261	6.4	0.313	7.6

MT2016-T11-50	50	T11	0.015	0.6	0.027	1.1	0.042	1.7
MT2016-T11-60	60	T11	0.042	1.2	0.074	2.1	0.116	3.2
MT2016-T12-03	3	T12	0.033	0.9	0.029	0.8	0.062	1.7
MT2016-T12-06	6	T12	0.056	1.2	0.049	1.0	0.105	2.2
MT2016-T12-09	9	T12	0.071	1.4	0.047	1.0	0.118	2.4
MT2016-T12-12	12	T12	0.063	1.9	0.042	1.3	0.105	3.1
MT2016-T12-15	15	T12	0.076	1.7	0.054	1.2	0.13	2.9
MT2016-T12-20	20	T12	0.07	1.7	0.922	22.9	0.992	24.3
MT2016-T12-30	30	T12	0.085	2.4	0.851	24.2	0.936	26.0
MT2016-T12-40	40	T12	0.162	2.9	0.945	17.1	1.107	19.5
MT2016-T12-50	50	T12	0.145	3.4	0.168	4.0	0.313	7.2
MT2016-T12-60	60	T12	0.188	3.9	0.078	1.7	0.266	5.5
MT2016-T13-03	3	T13	0.025	0.8	0.035	1.2	0.06	2.0
MT2016-T13-06	6	T13	0.077	1.4	0.24	4.5	0.317	5.9
MT2016-T13-09	9	T13	0.059	1.3	0.156	3.4	0.215	4.7
MT2016-T13-12	12	T13	0.039	1.2	0.087	2.6	0.126	3.7
MT2016-T13-15	15	T13	0.062	1.5	0.293	7.0	0.355	8.4
MT2016-T13-20	20	T13	0.125	2.1	1.066	18.1	1.191	19.8
MT2016-T13-30	30	T13	0.065	2.2	0.499	17.0	0.564	18.8
MT2016-T13-40	40	T13	0.075	1.3	0.197	3.5	0.272	4.7
MT2016-T14-03	3	T14	0.069	1.2	0.42	7.4	0.489	8.5
MT2016-T14-06	6	T14	0.083	1.6	0.165	3.3	0.248	4.9
MT2016-T14-09	9	T14	0.066	1.5	0.087	2.0	0.153	3.5
MT2016-T14-12	12	T14	0.132	2.5	0.137	2.7	0.269	5.2
MT2016-T14-15	15	T14	0.083	2.9	0.065	2.3	0.148	5.2
MT2016-T14-20	20	T14	0.143	3.6	1.337	34.7	1.48	37.0
MT2016-T14-30	30	T14	0.125	2.9	1.192	28.5	1.317	30.6
MT2016-T14-40	40	T14	0.091	2.7	0.667	20.1	0.758	22.2
MT2016-T15-03	3	T15	0.074	1.9	0.061	1.6	0.135	3.4

MT2016-T15-06	6	T15	0.245	8.8	0.049	1.9	0.294	10.6
MT2016-T15-09	9	T15	0.289	10.6	0.032	1.3	0.321	11.7
MT2016-T15-12	12	T15	0.275	7.6	0.045	1.3	0.32	8.8
MT2016-T15-15	15	T15	0.26	8.2	0.019	0.7	0.279	8.8
MT2016-T15-20	20	T15	0.278	6.5	0.041	1.0	0.319	7.5
MT2016-T15-30	30	T15	0.135	3.1	0.737	17.7	0.872	20.3
MT2016-T15-40	40	T15	0.172	2.9	0.726	12.6	0.898	15.1
MT2015-T2-03	3	T2	0.08	2.1	0.021	0.6	0.101	2.6
MT2015-T2-06	6	T2	0.127	3.3	0.033	0.9	0.16	4.1
MT2015-T2-09	9	T2	0.21	4.9	0.047	1.2	0.257	6.0
MT2015-T2-12	12	T2	0.169	6.2	0.034	1.3	0.203	7.4
MT2015-T2-15	15	T2	0.221	6.6	0.041	1.3	0.262	7.8
MT2015-T2-20	20	T2	0.191	5.7	0.059	1.9	0.25	7.4
MT2015-T2-30P-B	30	T2	0.127	3.2	0.715	18.4	0.842	21.0
MT2015-T2-40P-B	40	T2	0.081	2.2	0.574	16.2	0.655	18.1
MT2015-T2-50P	50	T2	0.055	2.5	0.057	2.3	0.112	5.0
MT2015-T2-60P	60	T2	0.044	2.1	0.047	2.2	0.091	4.4
LT2015-MT3-3D	3	T3	0.028	1.2	0.047	3.8	0.075	3.3
MT2015-T3-06	6	T3	0.074	2.1	0.229	6.5	0.303	8.5
LT2015-MT3-9D	9	T3	0.096	4.4	0.291	6.6	0.387	17.7
LT2015-MT3-12D	12	T3	0.099	4.4	0.25	5.7	0.349	15.5
LT2015-MT3-15D	15	T3	0.092	4.4	0.141	3.2	0.233	11.2
LT2015-MT3-20D	20	T3	0.096	5.3	0.256	4.8	0.352	19.6
MT2015-T3-30PB	30	T3	0.074	3.4	0.253	7.5	0.327	15.0
LT2015-MT3-40PA	40	T3	0.09	3.4	0.247	7.3	0.337	12.6
MT2015-T4-03	3	T4	0.032	0.7	0.055	1.2	0.087	2.0
MT2015-T4-06	6	T4	0.083	1.7	0.621	12.7	0.704	14.1
MT2015-T4-09	9	T4	0.08	1.5	0.484	9.4	0.564	10.8

MT2015-T4-12	12	T4	0.112	4.5	0.779	32.5	0.891	35.5
MT2015-T4-30P-B	30	T4	0.105	2.9	0.791	22.9	0.896	25.1
MT2015-T4-50P	50	T4	0.117	3.1	0.292	8.1	0.409	10.9
MT2015-T4-60P	60	T4	0.108	2.9	0.185	5.2	0.293	8.0
MT2015-T5-03	3	T5	0.125	3.4	0.029	0.8	0.154	4.2
LT2015-MT5-6D	6	T5	0.075	3.1	0.134	4.4	0.209	8.5
LT2015-MT5-9D	9	T5	0.119	4.7	0.039	0.8	0.158	6.2
LT2015-MT5-12D	12	T5	0.169	5.7	0.084	1.5	0.253	8.5
LT2015-MT5-15D	15	T5	0.099	3.9	0.193	5.0	0.292	11.4
LT2015-MT5-20D	20	T5	0.089	4.3	0.493	11.4	0.582	28.3
MT2015-T5-30P-A	30	T5	0.1	3.0	1.294	40.0	1.394	41.8
MT2015-T5-40P-B	40	T5	0.051	1.7	0.736	24.3	0.787	25.5
MT2015-T6-06	6	T6	0.386	8.5	0.832	20.1	1.218	26.9
LT2015-MT6-9D	9	T6	0.066	2.6	0.316	12.0	0.382	15.2
MT2015-T6-12	12	T6	0.129	4.5	1.005	36.9	1.134	39.7
LT2015-MT6-15D	15	T6	0.077	3.8	0.618	16.5	0.695	33.9
LT2015-MT6-20D	20	T6	0.062	2.6	0.394	15.3	0.456	19.0
MT2015-T6-30P	30	T6	0.097	2.6	1.063	29.4	1.16	31.3
MT2015-T6-40P	40	T6	0.049	2.1	0.05	2.4	0.099	4.2
MT2015-T6-50P	50	T6	0.116	2.8	0.789	19.7	0.905	22.0
MT2015-T6-60P	60	T6	0.147	3.7	1.095	28.4	1.242	31.1
MT2015-T7-03	3	T7	0.051	0.9	0.136	2.5	0.187	3.5
MT2015-T7-06	6	T7	0.071	1.5	0.419	9.2	0.49	10.6
MT2015-T7-09	9	T7	0.08	3.8	0.475	23.3	0.555	26.2
MT2015-T7-12	12	T7	0.157	6.5	0.629	27.9	0.786	32.6
MT2015-T7-15	15	T7	0.038	1.4	0.714	26.1	0.752	27.1
MT2015-T7-20	20	T7	0.121	3.2	0.953	26.0	1.074	28.4
MT2015-T7-30P-A	30	T7	0.1	3.2	1.142	38.1	1.242	40.1
MT2015-T7-40P	40	T7	0.09	4.2	0.253	12.2	0.343	15.9

MT2016-T8-03	3	T8	0.042	0.7	0.105	1.7	0.147	2.4
MT2016-T8-06	6	T8	0.036	0.8	0.11	2.4	0.146	3.1
MT2016-T8-09	9	T8	0.032	0.9	0.067	1.8	0.099	2.7
MT2016-T8-12	12	T8	0.042	1.1	0.084	2.2	0.126	3.3
MT2016-T8-15	15	T8	0.069	1.7	0.05	1.3	0.119	3.0
MT2016-T8-20	20	T8	0.079	2.2	0.05	1.4	0.129	3.6
MT2016-T8-30-2	30	T8	0.061	1.6	0.367	9.9	0.428	11.4
MT2016-T9-03	3	T9	0.043	1.1	0.11	3.0	0.153	4.1
MT2016-T9-09	9	T9	0.03	1.1	0.091	3.5	0.121	4.6
MT2016-T9-12	12	T9	0.054	1.2	0.086	2.0	0.14	3.2
MT2016-T9-15	15	T9	0.026	0.9	0.05	1.8	0.076	2.7
MT2016-T9-30	30	T9	0.036	1.0	0.194	5.6	0.23	6.6
MT2016-T9-40	40	T9	0.029	0.8	0.135	3.9	0.164	4.7
MT2015-T7-40P-A	NO SAMPLE TAKEN ONLY BIG SHELLS							
MT2015 Live Neoth.			0.195	**5.8**	0.026	**0.8**	0.221	**6.6**
MT2015-TLA-03	3	TLA	0.144	**3.9**	0.027	**0.8**	0.171	**4.7**
MT2015-TLA-06	6	TLA	0.222	**6.4**	0.033	**1.0**	0.255	**7.3**
MT2015-TLA-09	9	TLA	0.262	**6.7**	0.035	**1.0**	0.297	**7.7**
MT2015-TLA-12	12	TLA	0.217	**5.7**	0.035	**1.0**	0.252	**6.6**
MT2015-TLA-15	15	TLA	0.162	**3.8**	0.035	**0.9**	0.197	**4.6**
MT2015-TLA-20	20	TLA	0.188	**4.9**	0.034	**0.9**	0.222	**5.8**

Appendix G: LPSA Mud-Fraction Grain Size Data Summary

Sample Name	Depth	Transect	Dx (10)	Dx (50)	Dx (90)	Mode
Average of 'MT2016-LAR-5'		Onshore	0.094514	3.0326	16.01156	4.230844
Average of '2016-KbR-mud-2'		Onshore	2.386082	8.708011	34.04386	6.415675
Average of '2016-KbR-mud-1'		Onshore	2.65279	9.462374	36.18428	7.049392
Average of 'MT2016-LAR-3'		Onshore	3.053801	11.14305	40.09429	9.773668
Average of 'MT2015-LAR-5'		Onshore	3.339311	12.9169	51.59776	10.36372
Average of '2016-KbR-mud-6'		Onshore	3.642817	11.73155	34.6795	12.38079
Average of 'MT2015-LAR-2'		Onshore	2.938822	10.75057	35.76601	15.1422
Average of 'MT2015-LAR-4'		Onshore	3.489074	13.39625	42.24974	17.65941
Average of 'MT2015-LAR-3'		Onshore	3.434818	13.12359	39.29892	18.00779
Average of 'MT2015-LAR-1'		Onshore	3.452037	13.29176	39.44677	18.75903
Average of 'MT2016-LAR-1'		Onshore	3.213385	13.03921	43.05855	19.96099
Average of '2016-KbR-3'		Onshore	3.901523	16.34204	49.90197	22.5138
Average of '2016-KbR-RM-2'		Onshore	3.874701	17.00588	50.07336	26.3409
Average of '2016-KbR-RM'		Onshore	3.710934	18.74055	50.96829	27.52047
Average of '2016-Ngk-3'		Onshore	2.348384	12.02797	48.09338	28.85023
Average of '2016-Beach-1'		Onshore	4.543186	18.63471	47.8733	30.23257
Average of '2016-KbR-5'		Onshore	3.868754	17.29372	56.39722	30.23906
Average of '2016-Ngk-1'		Onshore	2.598276	12.94405	50.41836	31.19661
Average of 'MT2016-LAR-2'		Onshore	2.630774	14.31505	49.84544	32.76595
Average of '2016-KbR-9'		Onshore	4.421967	20.1319	61.129	37.28876
Average of '2016-KbR-mud-5'		Onshore	3.614108	17.80969	60.15685	40.92597
Average of '2016-KbR-mud-4'		Onshore	3.615804	19.43954	61.34374	41.12169
Average of '2016-KbR-4'		Onshore	4.484079	23.23454	65.06372	41.66323
Average of '2016-KbR-8'		Onshore	4.57625	23.15971	67.71719	42.0557
Average of '2016-KbR-2'		Onshore	4.269656	24.34728	66.14757	42.59874

Average of 'MT2015-Live Neoth. Site'		Onshore	5.091554	27.67148	66.18159	43.62206
Average of 'MT2015-TLA-15'		Onshore	4.547018	27.9974	65.74786	43.64055
Average of '2016-Ngk-2'		Onshore	3.408533	19.54094	65.64006	43.95609
Average of '2016-KbR-6'		Onshore	4.932229	29.4578	68.63001	44.94119
Average of '2016-KbR-1'		Onshore	4.841665	26.15496	70.05568	45.72721
Average of '2016-KbR-10'		Onshore	5.285241	32.61291	71.69062	46.87223
Average of '2016-KbR-mud-3'		Onshore	4.087977	27.82093	69.74694	46.89823
Average of '2016-KbR-7'		Onshore	4.652258	29.69087	70.68278	47.03162
Average of 'MT2016-LAR-4'		Onshore	4.534971	42.48157	84.82461	57.33297
Average of 'MT2015-T1-03'	3	T1	3.775619	12.02414	44.95155	9.589788
Average of 'MT2015-T1-06'	6	T1	6.533112	17.65158	42.51151	18.79239
Average of 'LT2015-MT1-9D'	9	T1				22.2
Average of 'LT2015-MT1-12D'	12	T1				12.8
Average of 'LT2015-MT1-15D'	15	T1				13.6
Average of 'MT2015-T1-20'	20	T1	4.887935	14.64112	45.00617	14.0175
Average of 'MT2015-T1-30PB'	30	T1				11.1
Average of 'MT2015-T1-40P-B'	40	T1	4.249657	11.88492	37.99231	11.33519
Average of 'MT2016-T10-03'	3	T10	5.232843	28.94017	73.41143	48.02187
Average of 'MT2016-T10-06'	6	T10	5.912532	32.9801	69.74993	44.38425
Average of 'MT2016-T10-09'	9	T10	5.91627	31.4131	66.4317	42.54912
Average of 'MT2016-T10-12'	12	T10	5.907683	30.18046	64.51833	40.78811
Average of 'MT2016-T10-15'	15	T10	5.461228	30.37178	65.02734	41.69025
Average of 'MT2016-T10-20'	20	T10	6.423797	32.35546	65.75318	41.7116
Average of 'MT2016-T10-30'	30	T10	7.160749	33.48423	64.70553	40.64525
Average of 'MT2016-T10-40'	40	T10	8.156423	36.87867	69.57809	43.27225
Average of 'MT2016-T11-03'	3	T11	7.351781	32.52886	116.4624	38.3049
Average of 'MT2016-T11-06'	6	T11	6.092409	18.29902	54.70186	17.53811
Average of 'MT2016-T11-09'	9	T11	6.226337	22.63633	64.34437	30.60007
Average of 'MT2016-T11-12'	12		5.625598	27.31954	68.89296	45.74302

Average of 'MT2016-T11-15'	15	T11	5.904137	23.23379	70.74585	50.13055
Average of 'MT2016-T11-20'	20	T11	6.688642	41.8554	81.4507	55.02428
Average of 'MT2016-T11-30'	30	T11	7.317354	34.96256	74.82073	50.14429
Average of 'MT2016-T11-40'	40	T11	6.157154	29.40217	71.16042	45.81418
Average of 'MT2016-T11-50'	50	T11	5.022968	19.81529	65.71426	35.36963
Average of 'MT2016-T11-60'	60	T11	5.308128	20.10247	57.93425	33.84765
Average of 'MT2016-T12-03'	3	T12	7.943594	36.78978	75.30534	48.18702
Average of 'MT2016-T12-06'	6	T12	9.356728	38.03895	74.52466	47.42959
Average of 'MT2016-T12-09'	9	T12	9.964918	40.19682	72.57227	46.21302
Average of 'MT2016-T12-12'	12	T12	11.79983	39.52421	70.4849	44.8286
Average of 'MT2016-T12-15'	15	T12	16.02083	40.55627	70.98151	44.63597
Average of 'MT2016-T12-20'	20	T12	12.28946	40.11591	73.12352	46.08557
Average of 'MT2016-T12-30'	30	T12	7.128592	33.36736	65.74176	41.12887
Average of 'MT2016-T12-40'	40	T12	7.077351	33.93217	67.23861	42.17784
Average of 'MT2016-T12-50'	50	T12	5.791845	24.25565	57.82749	31.95787
Average of 'MT2016-T12-60'	60	T12	6.327169	28.43987	58.66822	35.53527
Average of 'MT2016-T13-03'	3	T13	7.713693	28.93978	72.10743	44.73577
Average of 'MT2016-T13-06'	6	T13	6.510724	41.14821	81.88425	54.19056
Average of 'MT2016-T13-09'	9	T13	6.105281	38.67011	78.38697	52.41948
Average of 'MT2016-T13-12'	12	T13	8.018814	41.70472	79.04609	52.13889
Average of 'MT2016-T13-15'	15	T13	8.871674	45.52589	80.12136	52.32875
Average of 'MT2016-T13-20'	20	T13	9.15426	47.00318	81.99217	53.453
Average of 'MT2016-T13-30'	30	T13	7.721443	40.23675	81.12736	53.77023
Average of 'MT2016-T13-40'	40	T13	7.74506	41.10185	76.63979	49.36519
Average of 'MT2016-T14-06'	6	T14	4.890755	32.50759	75.07842	50.13323
Average of 'MT2016-T14-09'	9	T14	5.053555	37.4635	79.37922	54.14385
Average of 'MT2016-T14-12'	12	T14	5.614724	40.73535	77.73556	51.36921
Average of 'MT2016-T14-15'	15	T14	6.381285	42.19518	77.27417	50.67675
Average of 'MT2016-T14-20'	20	T14	3.399477	19.12392	62.84648	43.03956

Average of 'MT2016-T14-03'	3	T14	5.097889	22.43171	144.3609	24.80287
Average of 'MT2016-T14-30'	30	T14	2.469482	9.234268	44.00189	6.013948
Average of 'MT2016-T14-40'	40	T14	2.757421	10.58255	39.65686	7.598251
Average of 'MT2016-T15-03'	3	T15	3.111749	16.40549	42.45375	24.16584
Average of 'MT2016-T15-06'	6	T15	4.191629	29.51993	64.54054	41.75292
Average of 'MT2016-T15-09'	9	T15	4.044349	27.14568	60.4738	38.81734
Average of 'MT2016-T15-12'	12	T15	3.493858	21.11433	55.00241	33.59388
Average of 'MT2016-T15-15'	15	T15	3.312486	20.03112	52.79656	32.27027
Average of 'MT2016-T15-20'	20	T15	4.797437	27.21977	58.87573	36.51296
Average of 'MT2016-T15-30'	30	T15	3.402721	17.96816	54.19592	32.96621
Average of 'MT2016-T15-40'	40	T15	4.027989	20.78839	65.29482	37.72075
Average of 'MT2015-T2-03'	3	T2	3.978382	19.14545	54.86018	30.14001
Average of 'MT2015-T2-06'	6	T2	4.817014	27.85489	68.84299	45.22493
Average of 'MT2015-T2-09'	9	T2	6.258402	35.06461	68.54794	43.73281
Average of 'MT2015-T2-12'	12	T2	7.277323	33.94305	66.55706	41.55656
Average of 'MT2015-T2-15'	15	T2	6.012808	33.17363	66.40211	42.09165
Average of 'LT20105-MT2-15D'	15	T2				31.2
Average of 'LT20105-MT2-20D'	20	T2				35.4
Average of 'MT2015-T2-30'	30	T2	4.165444	19.89705	53.81934	30.74782
Average of 'MT2015-T2-40'	40	T2	4.104855	14.40025	45.45726	20.05679
Average of 'MT2015-T2-50P'	50	T2				10.3
Average of 'MT2015-T2-60P'	60	T2				11.4
Average of 'LT2015-MT3-3D'	3	T3				15.1
Average of 'LT20105-MT3-9D'	9	T3				22
Average of 'LT2015-MT3-12D'	12	T3				27.5
Average of 'LT2015-MT3-20D’	20	T3				29.5
Average of 'MT2015-T3-30PB'	30	T3				15.1
Average of 'LT2015-MT3-40PA’	40	T3				9.78
Average of 'MT2015-T4-03'	3	T4	4.619494	19.05573	61.96576	39.77766

Average of 'MT2015-T4-06'	6	T4	5.355399	15.46914	49.83183	13.7504
Average of 'MT2015-T4-09'	9	T4	5.362281	15.23064	43.91735	14.39995
Average of 'MT2015-T4-12'	12	T4	4.469128	18.65826	58.90522	24.49904
Average of 'MT2015-T4-15'	15	T4	4.786116	19.90651	60.36879	25.13973
Average of 'MT2015-T4-20'	20	T4	5.806467	22.48428	71.51792	24.88046
Average of 'MT2015-T4-30P-B'	30	T4	3.999119	14.00543	52.13181	9.769391
Average of 'MT2015-T4-40P-B'	40	T4	4.831396	19.04287	46.01403	24.70735
Average of 'MT2015-T4-50P'	50	T4	3.976193	14.81298	50.17568	22.70282
Average of 'MT2015-T4-60P'	60	T4	3.660763	15.34954	59.35914	26.26522
Average of 'MT2015-T5-03'	3	T5	7.016222	36.73354	70.86418	46.5169
Average of 'MT2015-T5-06'	6	T5	5.239709	25.15479	57.24391	35.80325
Average of 'MT2015-T5-06'	6		7.13502	43.11757	80.00017	53.09756
Average of 'MT2015-T5-09'	9	T5	5.729439	29.09857	61.73283	37.89143
Average of 'MT2015-T5-12'	12	T5	4.742542	23.76227	55.35193	34.45606
Average of 'MT2015-T5-15'	15	T5	4.270397	14.88696	45.90023	14.36353
Average of 'MT2015-T5-20'	20	T5	3.950659	12.2142	37.90954	11.47306
Average of 'MT2015-T5-30P-A'	30	T5	5.781481	23.03757	71.20964	27.13843
Average of 'MT2015-T5-40P-B'	40	T5	6.029967	22.75081	78.43156	22.63777
Average of 'LT20105-T6-3D’	3	T6				13.4
Average of 'MT2015-T6-06'	6	T6	9.750119	42.87472	76.35664	49.29346
Average of 'MT2015-T6-09'	9	T6	7.139269	31.73444	67.85242	43.19092
Average of 'MT2015-T6-12'	12	T6	6.915415	36.89671	75.21767	48.41552
Average of 'MT2015-T6-15'	15	T6	8.08927	30.45358	83.3162	35.96967
Average of 'MT2015-T6-20'	20	T6	4.243492	15.0962	50.55469	12.91834
Average of 'MT2015-T6-30P'	30	T6	4.584065	19.6202	61.63292	38.05426
Average of 'MT2015-T6-40P'	40	T6	4.39614	12.92562	39.87851	12.12173
Average of 'MT2015-T6-50P'	50	T6	4.366277	16.37864	49.94476	21.94645
Average of 'MT2015-T6-60P'	60	T6	4.478658	15.56446	50.23309	15.82257
Average of 'MT2015-T7-03'	3	T7	5.984235	21.68352	71.95581	51.71472

Average of 'MT2015-T7-06'	6	T7	6.548484	23.7782	64.19051	40.0644
Average of 'MT2015-T7-09'	9	T7	6.476818	29.85657	65.47233	40.82248
Average of 'MT2015-T7-12'	12	T7	5.486981	26.42758	66.52405	42.9449
Average of 'MT2015-T7-15'	15	T7	4.46923	21.28976	59.85144	40.35171
Average of 'MT2015-T7-20'	20	T7	5.938865	27.80227	67.3762	43.03987
Average of 'MT2015-T7-30P-A'	30	T7	6.196607	22.47069	62.72236	35.37425
Average of 'MT2015-T7-40P-A'	40	T7	5.681704	28.27571	65.9619	40.51911
Average of 'MT2016-T8-03'	3	T8	5.423693	21.03772	55.31075	29.6784
Average of 'MT2016-T8-06'	6	T8	5.185834	23.96542	70.48043	38.39969
Average of 'MT2016-T8-09'	9	T8	5.613907	20.07982	59.588	22.33425
Average of 'MT2016-T8-12'	12	T8	4.986124	28.79324	70.93385	46.29527
Average of 'MT2016-T8-15'	15	T8	5.356729	37.05752	76.04452	50.99106
Average of 'MT2016-T8-20'	20	T8	6.300481	40.60941	79.30919	52.4633
Average of 'MT2016-T8-30'	30	T8	9.085599	44.07918	78.43467	50.79828
Average of 'MT2016-T8-40-2'	40	T8	6.032312	24.69628	93.16387	22.43707
Average of 'MT2016-T9-03'	3	T9	6.791969	31.65731	218.6295	33.03968
Average of 'MT2016-T9-09'	9	T9	6.464066	28.84968	73.94399	41.70847
Average of 'MT2016-T9-12'	12	T9	5.535264	31.22428	74.42194	45.96151
Average of 'MT2016-T9-15'	15	T9	6.071315	37.04047	124.1954	49.09373
Average of 'MT2016-T9-30'	30	T9	6.191705	26.93494	67.43346	42.63318
Average of 'MT2016-T9-40'	40	T9	5.165688	20.06637	57.02331	31.23429
Average of 'MT2015-TLA-03'	3	TLA	3.22878	16.21652	54.26877	34.44083
Average of 'MT2015-TLA-06'	6	TLA	2.918786	11.90637	38.64134	18.3893
Average of 'MT2015-TLA-09'	9	TLA	3.443438	14.29216	43.91801	23.09805
Average of 'MT2015-TLA-12'	12	TLA	3.912679	19.45224	56.70501	36.05214
Average of 'MT2015-TLA-20'	20	TLA	3.346713	17.63442	51.35622	31.5573